BULLETIN OF THE EARTHQUAKE
RESEARCH INSTITUTE
Vol. 58 (1983), pp. 65-134

3. *Waveform and Spectral Features of Earthquake Swarms and Foreshocks*

—in Special Reference to Earthquake Prediction—

By Masaru TSUJIURA,
Earthquake Research Institute.

(Received January 31, 1983)

Abstract

Through the analyses of waveforms and spectra for the earthquake swarm, foreshock and ordinary seismic activities, some differences in the activity mode are found among those activities. The most striking difference is the "similarity of waveform". The earthquake swarm activity which occurred in a certain short time interval mainly consists of events with similar waveforms, belonging to the event group called "similar earthquakes" or an "earthquake family". On the other hand, the foreshock activity consists of events with an individual waveform character. Similarly, the rate of the occurrence of earthquake families is very low in ordinary seismic activity. The epicenters of earthquakes in a family are distributed within a small area, about 400 meters for a family with $M_{max} \cong 3.0$, in contrast with a wide area for foreshocks. The source spectra of earthquake swarms also show some features differing from those of other activities. The corner frequencies of events in the same family are almost constant, and their values depend on the size of the largest earthquake within the family. On the other hand, the corner frequencies of foreshocks differ from event to event, and there is no simple linear relation between the corner frequency and the earthquake size. Such behavior suggests that the earthquakes in a family occur on the same fault plane as a repeated slipping or a repeated incomplete rupture, and foreshocks occur independently in a heterogeneous zone near the main shock. If such differences are applicable for the other sequences, continuous monitoring of waveforms and spectra gives us some useful information for distinguishing a foreshock sequence from an earthquake swarm.

TABLE OF CONTENTS

page

CHAPTER 1 Introduction 66
CHAPTER 2 Interpretation of Earthquake Swarms 69
CHAPTER 3 Data 71
3.1. General description of seismograph system 71

3.2. Spectrum analyzing seismograph 74
3.3. Triggered seismogram 76
CHAPTER 4 Waveform Analysis of Earthquake Swarms 76
4.1. Introduction 76
4.2. Method of analysis 77
4.3. Waveform feature of earthquake swarms 78
4.3a. Earthquake swarm off Kawanazaki, Izu Peninsula in 1978 78
4.3b. Earthquake swarm in northern Tokyo Bay in 1979 80
4.3c. Earthquake swarm off the east coast of the Izu Peninsula in 1980 82
4.3d. Other earthquake swarms 86
4.4. Spatial distribution of swarm earthquakes 89
4.5. Conclusion 92
CHAPTER 5 Spectral Analysis of Earthquake Swarms 93
5.1. Introduction 93
5.2. Method of analysis 93
5.3. Spectral feature of earthquake swarms 94
5.4. Scaling law of source spectrum 95
5.4a. Earthquake swarm off Kawanazaki, Izu Peninsula in 1978 98
5.4b. Earthquake swarm in northern Tokyo Bay in 1979 101
5.4c. Earthquake swarm off the east coast of the Izu Peninsula in 1980 102
5.5. Prediction of the largest earthquake 109
5.6. Conclusion 115
CHAPTER 6 Differences in the Activity Mode between Earthquake Swarm and Other Seismic Activities 116
6.1. Introduction 116
6.2. Waveform feature of foreshocks 116
6.3. Spectral feature of foreshocks 121
6.4. Local variation of source spectra 123
6.5. Earthquake family in ordinary seismic activity .. 124
6.6. Conclusion 126
CHAPTER 7 Concluding Remarks 126
REFERENCES 129

CHAPTER 1

Introduction

The earthquakes occurring prior to the pricipal earthquake are usually called "foreshocks". ŌMORI (1910) and IMAMURA (1913, 1915) investigated the earthquakes preceded by foreshocks from various data available at that time and pointed out that such earthquakes were liable to occur in some limited regions.

MOGI (1963b) studied the frequency of foreshocks using the data of the Japan Meteorological Agency from 1926 to 1961 and pointed out that 4 per cent of shallow earthquakes with magnitudes (M) greater than 4 were preceded by foreshocks. A similar study was made by JONES and MOLNAR (1976) using world-wide data from 1950 to 1973 and pointed out that 44 per cent of large shallow earthquakes ($M \geqq 7.0$) were preceded by foreshocks. Recent observations with high magnification seismographs will be expected to detect foreshocks at a much higher rate. In fact, many small foreshocks were detected even in moderate-size earthquakes with $M \cong 5.5$ (UCHIIKE and ICHIKAWA, 1976; TSUMURA *et al.*, 1977; SUZUKI, 1981).

On the other hand, it is well known that there are earthquake swarms which are not accompanied by a principal earthquake. When the seismic activity in a certain region is increasing abruptly, it is very important to distinguish whether these earthquakes are foreshocks preceding a large earthquake or whether they are swarm earthquakes without a large earthquake. If a method for distinguishing these two types of activities is found, it will give an important clue for earthquake prediction. In fact, pronounced foreshock activity was one of the most useful information in the successful short-term prediction of the 1975 Haicheng, China earthquake (ZHENG, 1981).

Along this direction, some experiments have been made in terms of the frequency-magnitude relationship expressed by the "b" value. For example, SUYEHIRO (1966, 1969) and SUYEHIRO *et al.* (1964) found small b-values for some foreshock sequences compared with those of aftershocks and earthquake swarms, and they pointed out the possibility of distinguishing foreshocks from other activities. Similar small b-values were observed for the activity preceding the earthquake off east Hokkaido in 1968 (MOTOYA, 1970) and for the foreshock sequences of earthquakes which occurred in Greece (PAPAZACHOS, 1975). Such differences in b-value are also consistent with the laboratory experiments conducted by MOGI (1963b) and SCHOLZ (1968). However, some authors do not agree that the b-values of foreshocks are always smaller than the b-values of aftershocks (UTSU, 1971). Some earthquake swarms along the Japan trench also show small b-values (UTSU, 1969).

On the other hand, from the waveform analysis of seismic waves, some kinds of spectral features associated with foreshocks were found for the earthquakes in certain regions. For example, the relative decrease of high frequency amplitudes was found for both P and S waves of small events preceding large earthquakes in the Kamchatka region (FEDOTOV *et al.*, 1972). The earthquakes with low stress drop were also found for the immediate foreshocks of moderate earthquakes

in the Kanto area (TSUJIURA, 1977). Contrary to these results, ISHIDA and KANAMORI (1980) pointed out that the frequency of spectral peak is higher for the foreshocks than for the events of ordinary background activity. However, BAKUN and MCEVILLY (1979) concluded that the predominant frequency of foreshocks are neither universally higher nor lower than comparable ordinary earthquakes. Similarly, complicated patterns of the source spectra were found in the foreshock sequence of the 1978 Izu-Oshima-kinkai earthquake (TSUJIURA, 1978b).

Recently, UTSU (1981) proposed a possibility of distinguishing foreshocks from the relation between the size of felt area and the magnitude of event concerned. The largest foreshock usually has a large felt area compared with those of ordinary events with comparable magnitudes. Such a relation suggests that the foreshocks abound in high frequency components which correspond to high stress drop events. However, the spectrum of seismic waves depends on seismic area and source depth (TSUJIURA, 1977, 1978a, 1978b; MASUDA, 1978). Local variations of the source spectrum and the effect of source depth must be taken into account for elucidating the felt area. Therefore, for the present case, any definitive conclusion have not yet been obtained for distinguishing foreshocks in terms of *b*-values or the spectral method.

In order to overcome the above difficulties, we shall attempt to clarify the nature of earthquake swarms on the basis of the waveform and spectral analyses. A paper by NASU *et al.* (1931) was the first study on earthquake swarms by instrumental observation. After that, numerous studies on earthquake swarms have been made, especially with regard to space-time distribution, frequency-magnitude relationship and focal mechanism solution, and they have been discussed in terms of the tectonic conditions of their regions (e.g., MOGI, 1963b; SYLVESTER *et al.*, 1970; WETMILLER, 1971; SBAR *et al.*, 1972; JOHNSON and HADLEY, 1976; KLEIN *et al.*, 1977; MITSUNAMI and KUBOTERA, 1977; GEDNEY *et al.*, 1980). However, we have not yet obtained any satisfactory knowledge about the inherent nature of earthquake swarms compared with foreshock activity and ordinary background seismicity.

The present paper consists of five chapters. We shall start, in Chapter 2, the criterion of the selection of earthquake swarms and, in Chapter 3, seismic data currently processed at our seismic observatory will be described. Fifteen earthquake swarms and three foreshock activities during the past 14 years were found in our data library. From detailed analyses of waveform and spectrum, in Chapters 4 and 5, we shall show significant waveform and spectral features of earthquake swarms closely relating to its activity mode. Finally, in Chapter 6, the difference in the activity mode between the earthquake swarm

and the foreshock activity or the ordinary seismicity will be described.

We hope that the work presented here will contribute to a better understanding of the nature of earthquake swarms and for distinguishing earthquake swarms from other seismic activities.

CHAPTER 2

Interpretation of Earthquake Swarm

Seismic activities which increase in a certain limited region are classified into several types. MOGI (1963b) distinguished the seismic activities into the following three types: (1) main shock-aftershocks, (2) foreshocks-main shock-aftershocks and (3) an earthquake swarm. The definitions of these types have not yet been established clearly. Some studies on this subject have been made by MOGI (1963a, 1963b), UTSU (1969, 1970, 1971) and YAMAKAWA (1966, 1967a, 1967b). Among these three types of activities, the earthquake sequence where the number and the magnitude of earthquakes increase gradually with time and decrease after a certain period without any distinct main shock is called an "earthquake swarm" (MOGI, 1963b).

On the basis of laboratory measurements and the seismicity pattern in Japan, MOGI (1963a, 1963b) suggested that the main shock-aftershock sequence occurs in homogeneous regions, and the swarm sequence is limited to regions where the material properties are remarkably heterogeneous and fractured. Laboratory studies of microfracturing also suggest a correlation between swarmlike sequences and material heterogeneities (SCHOLZ, 1968).

The pattern of the foreshock-main shock-aftershock sequence is an intermediate one between the main shock-aftershock and the earthquake swarm types, and it appears at regions of moderately heterogeneous structure (MOGI, 1963b). Mogi also pointed out that the second and the third type sequences frequently appear in the same region.

The time duration of earthquake swarm varies from a few hours to a few months and depends on the tectonic nature of the seismic region. In some special cases, such as the Matsushiro earthquake swarm, the activity continued for about five years (HAGIWARA and IWATA, 1968).

For the present study on earthquake swarms, the field of Kanto is selected because it, especially the Izu-Nagano region, is one of the most active areas of earthquake swarms (MOGI, 1963b; UTSU, 1981). In this area foreshock activities have been frequently found (TSUMURA *et al.*, 1978; UTSU, 1981). A comparison of the seismic property for both sequences therefore would provide valuable data for studying the

difference between them.

For the selection of earthquake swarms, the number of earthquakes, epicentral location, distribution of magnitude and their occurrence times are considered. We will only treat the earthquake swarm activity in which at least five earthquakes of similar magnitudes ($\Delta M < 1$) occur within an area of about $15 \times 15\,km^2$ and with a time interval of 10 hours. The ΔM used here means the difference of magnitude between the largest earthquake and the second largest earthquake in a given earthquake sequence.

From the monthly lists of earthquakes of the Japan Meteorological Agency (JMA) and the data library of our seismograph stations, 15 earthquake swarms having the fore-mentioned conditions were selected during the period from 1968 to 1981. Table 1 shows the list of earthquake swarms together with the event parameters taken from the monthly lists of JMA.

None of these swarm sequences include an especially large earthquake, except for the two swarm sequences which occurred off the east coast of the Izu Peninsula (Nos. 9, 14). The difference of magnitude between the largest and the second largest earthquake of these sequences is 1.3 for the No. 9 and 1.8 for the No. 14 swarm, respectively. According to the classification by UTSU (1981), such a case corresponds to the activity of "type 4" which shows a swarmlike sequence including a specially large earthquake. However, as inferred from the activity mode of these sequences, we refer to these sequences as an ordinary earthquake swarm (TSUJIURA, 1979a, 1981). These swarms, including the three foreshock activities in the Kanto area

Table 1. List of earthquake swarms. M^*; magnitude of the largest earthquake in each swarm sequence.

No.	Date	M^*	Area
1	1969 May 15-16	3.8	S. of Chiba Pref.
2	1972 Jan. 14	3.8	Near Oshima
3	1973 Jan. 20-27	5.2	S. E. off Boso Pen.
4	1973 Nov. 14	4.1	Near Oshima
5	1974 May 2-5	5.2	E. off Chiba Pref.
6	1975 June 4	4.2	C. Chiba Pref.
7	1978 Apr. 6-7	6.1	E. off Chiba Pref.
8	1978 July 27-28	5.1	Off Ibaraki Pref.
9	1978 Nov. 24-Dec. 10	5.4	N. Izu Peninsula
10	1979 Mar. 15-22	3.1	N. Izu Peninsula
11	1979 May 20-24	3.8	N. Izu Peninsula
12	1979 July 11-Aug. 3	3.2	N. Tokyo Bay
13	1979 July 24-25	4.2	Off Ibaraki Pref.
14	1980 June 24-July 28	6.7	Izu Peninsula
15	1981 May 4-5	3.2	Sagami Bay

and the ordinary seismic activity in a specified area of the Kanto district, are the materials of the present study.

CHAPTER 3

Data

3.1. General description of the seismograph system

The data used in this study was compiled mainly by the Dodaira Micro-earthquake Observatory (DDR) and its satellite stations. The locations of the seismographic stations with their local geology are shown in Fig. 3.1 and Table 2. All seismic signals are recorded at the Earthquake Research Institute, Tokyo (ERI), by the telemetering system developed by MIYAMURA and TSUJIURA (1955, 1957), TSUJIURA and MIYAMURA (1959) and TSUJIURA (1963). DDR is the main station of our seismic network. Since 1968, three kinds of instruments, i.e., short-period (SP), medium-period (MP) and long-period (LP, LP-Low gain) seismographs have been in operation. Moreover, since 1973, two types of seismographs with wide-band (WB) and ultra long-period (ULP) were added in order to cover a wider dynamic range. Figure

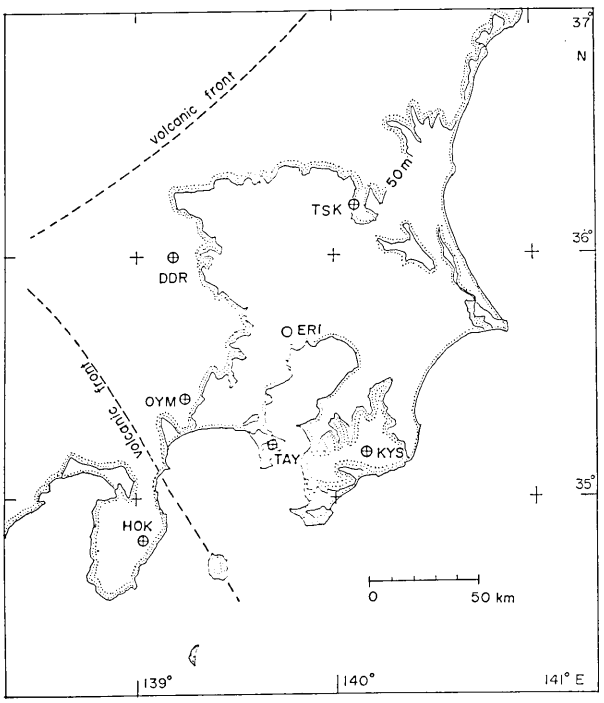

Fig. 3.1. Distribution of seismographic stations. All seismic signals are recorded at Earthquake Research Institute, Tokyo (ERI), by a telemetering system.

Table 2. List of seismographic stations with their local geology.

Station	Code	Location	Altitude	Rock type
		D M S	m	
Dodaira	DDR	35 59 54.0N 139 11 36.2E	800	Crystalline schist
Tsukuba	TSK	36 12 39.0N 140 06 35.0E	280	Granite
Kiyosumi	KYS	35 11 51.6N 140 08 53.6E	180	Sandstone (Tertiary shale)
Ohyama	OYM	35 25 12.3N 139 14 34.9E	600	Andesite
Hokiyama	HOK	34 50 59.4N 139 02 22.8E	890	Andesite
Takeyama	TAY	35 12 53.2N 139 39 34.2E	170	Basalt

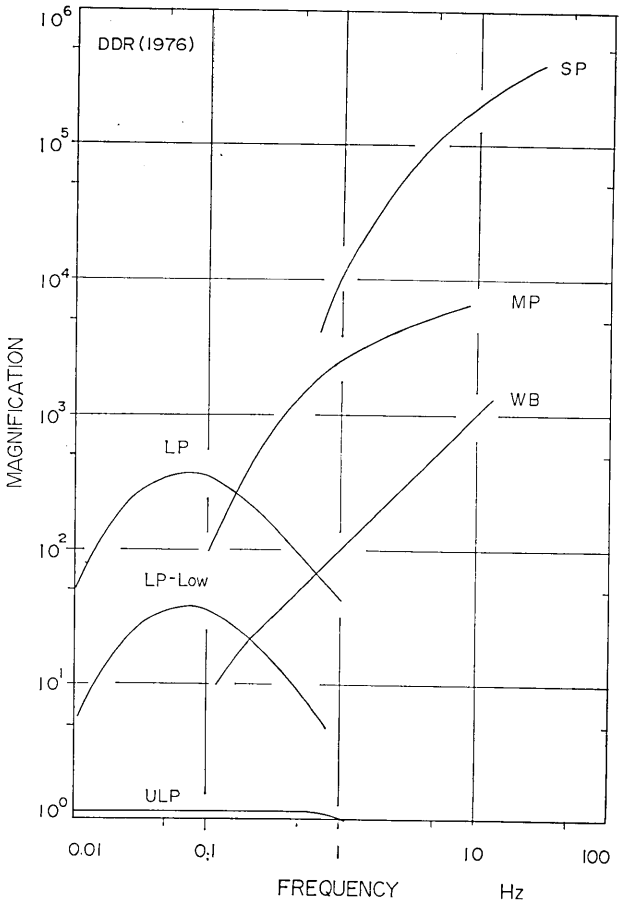

Fig. 3.2. Magnification curves of the seismographs at DDR. SP; short-period, MP; medium-period, WB; wide-band, LP; long-period, ULP; ultra long-period seismographs, respectively.

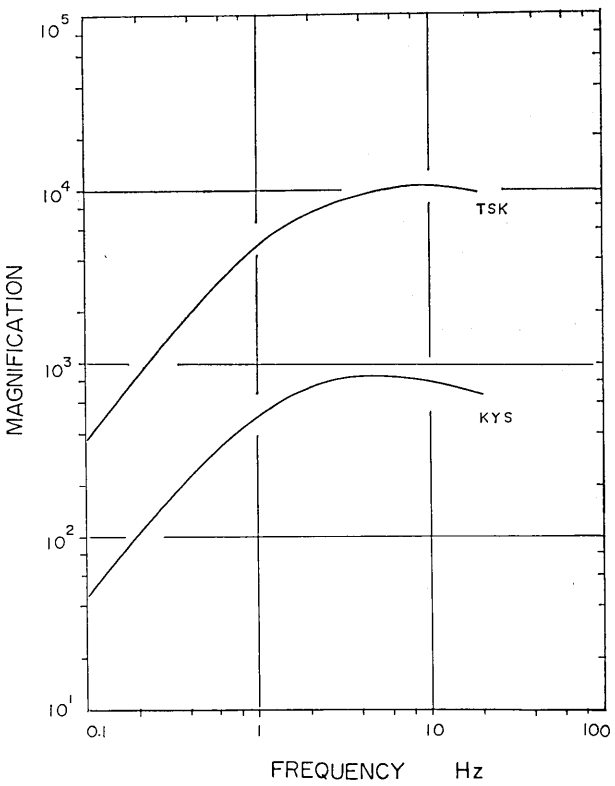

Fig. 3.3. Magnification curves of the medium-period seismographs at TSK and KYS.

3.2 shows the displacement magnification curves of these seismographs. A detailed description of the system was given by TSUJIURA (1965, 1967, 1973b).

In the recording station at ERI, all seismic signals which are observed at DDR, except for the signals of SP seismographs, have been continuously recorded on magnetic tape since the beginning of 1968. In these data, local earthquakes with magnitudes greater than about 3.5 are transcribed on a commercial 1/4 inch tape together with the teleseismic events with magnitudes (m_b) greater than about 5.5, and these tapes are preserved as a permanent data library.

The observation system at the Tsukuba (TSK) and Kiyosumi (KYS) stations consists of short-period and medium-period seismographs, while that at the other stations consists only of short-period seismographs. Since November of 1977, the signals of medium-period seismographs for both stations have also been recorded continuously on magnetic tape. The magnification curves of these seismographs are shown in Fig. 3.3. Moreover, since December of 1978, a magnetic tape recording system has been applied to the data of short-period seismographs for

all stations. This data is also available when necessary (TSUJIURA, 1980).

3.2. Spectral analyzing seismograph

In order to obtain the spectral contents of seismic waves an analog-type spectrum analyzer which consists of narrow band-pass filters has been operated on a routine basis (TSUJIURA, 1966, 1967, 1978a). An outline of the system will be described in the following.

The analyzer consists of one amplifier, six band-pass filters with center frequencies at 0.75, 1.5, 3, 6, 12 and 24 Hz and respective bandwidths of 0.5, 1, 2, 4, 8 and 16 Hz. In addition, high-frequency bands centered at 48 and 96 Hz with respective bandwidths of 32 and 64 Hz are used in some cases. The output of the six or eight filters is recorded continuously on an ink-writing 6 channel or 8 channel chart-recorder. The input of the amplifier is connected to the output of the

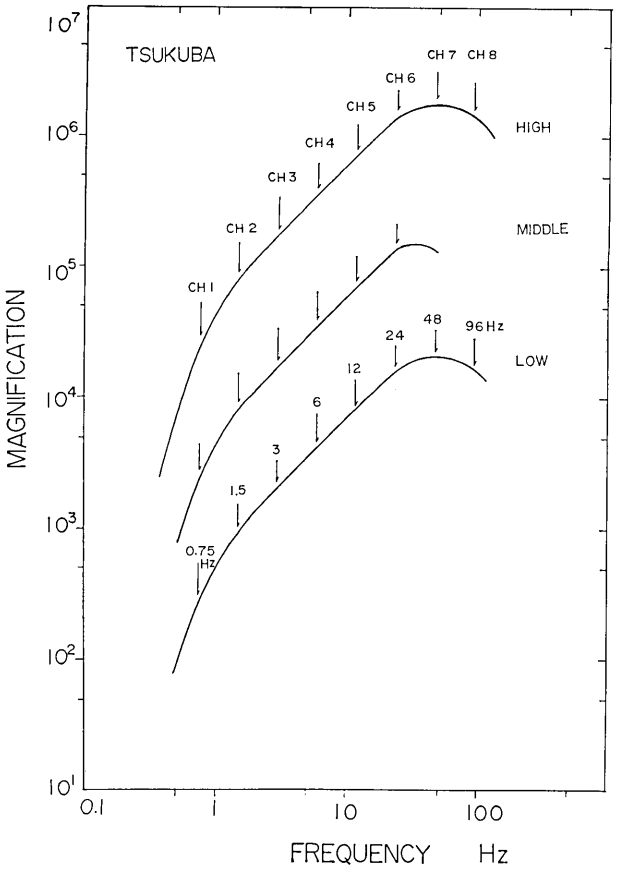

Fig. 3.4. Magnification curves of the short-period seismographs with band-pass filters at TSK. Arrows show the channel number of band-pass filters and its center frequency, respectively.

seismic telemetering network in the Kanto district. Three sets of identical analyzers have been in operation since 1976.

The displacement magnification curves of the seismographs at TSK station and the filter response, which has the same frequency characteristics for the three sets, are shown in Figs. 3.4 and 3.5, respectively. Since 1978, two sets of analyzers, except for the data of TSK marked as "middle", are connected to other stations. Figure 3.6 shows the displacement magnification curves when the analyzers are connected to the corresponding stations. The magnification of the seismographs at four stations differs from station to station. The combined data for these stations therefore cover a wide dynamic range of the spectrum up to 1.5 in a magnitude unit. In addition, as mentioned earlier, DDR has a magnetic tape recording system consisting of various kinds of seismographs. This data is also available for the analysis of large events ($M > 3.5$). Although our data give a rough estimation of the spectrum, it is useful when a great deal of data are processed (e.g., AKI, 1980a).

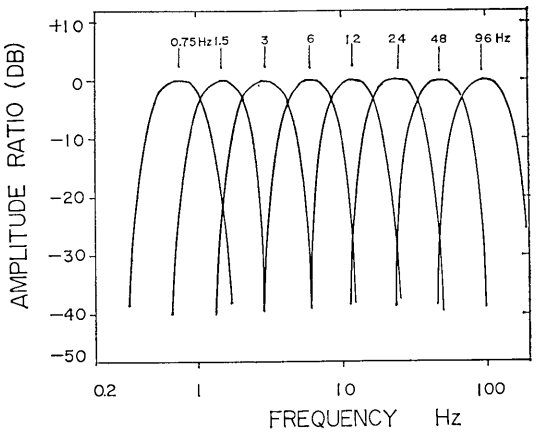

Fig. 3.5. Frequency response curves of band-pass filters used in the spectral analysis. The frequencies from 0.75 to 96 Hz indicate the center frequency of each band-pass filter.

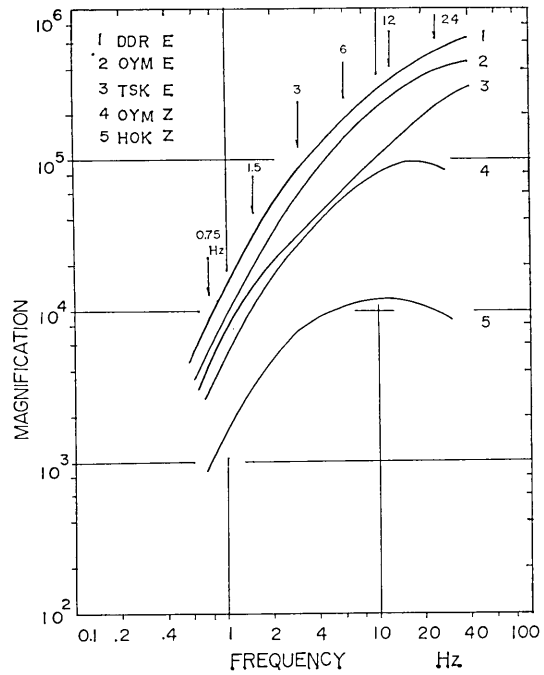

Fig. 3.6. Magnification curves of the short-period seismographs including band-pass filters. Arrows show the center frequencies of band-pass filters.

3.3. Triggered seismogram

For the waveform analysis, seismograms recording at a high paper speed (10–100 mm/sec) by a trigger mode are available. The observation of this system was started from November of 1978 at two stations, OYM and HOK. After that, the number of station increased, and at present, the data of five stations are available for the analysis of waveform (TSUJIURA, 1981).

CHAPTER 4

Waveform Analysis of Earthquake Swarms

4.1. Introduction

The earthquakes in a swarm sequence usually show a concentrated activity. Figure 4.1 shows a typical example of an earthquake swarm which consists of activities lasting about two hours. These seismograms were obtained at DDR ($\Delta \cong 150$ km) for the 1980 earthquake swarm off the east coast of the Izu Peninsula (TSUJIURA, 1981). Many earthquakes occur within a short time interval of one hour. Such a continual occurrence of earthquakes affects accuracy in determining epicenters, because the initial motions of P waves are contaminated by the coda waves of earlier events. Therefore, we try the waveform analysis using the triggered-seismograms in order to find the inherent

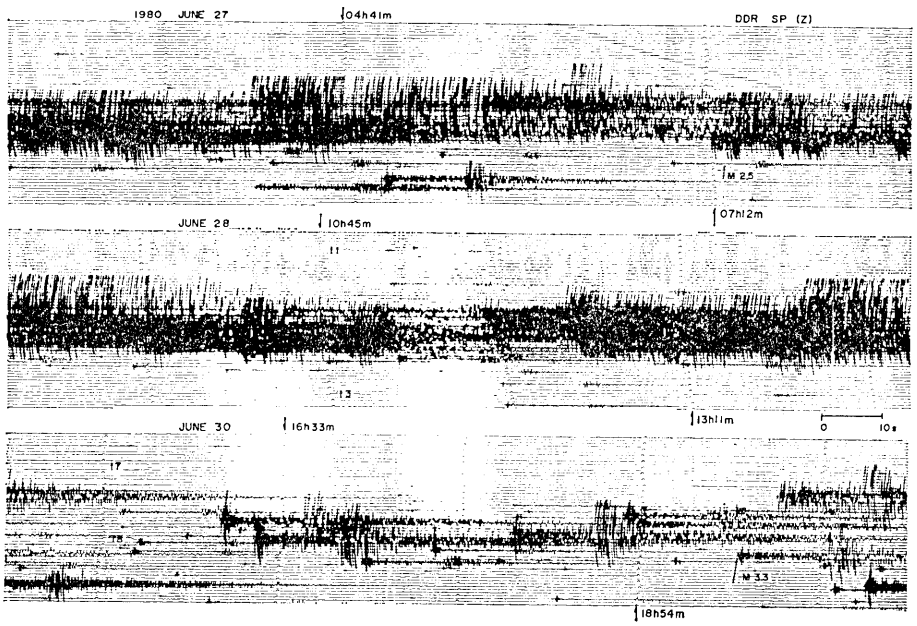

Fig. 4.1. Seismograms for three periods with concentrated activity obtained at DDR during the 1980 earthquake swarm off the east coast of the Izu Peninsula.

nature of the earthquake swarm. We shall show some features of waveforms which closely relate to the activity mode, such as the mechanism of earthquake occurrence, the distribution of epicenters and the migration of the activity area with time.

4.2. Method of analysis

The waveform analysis is performed by a visual examination of waveforms on the seismograms recorded at a high paper speed by a trigger mode (TRG). The paper speed of the TRG seismograms depends on the spectrum of seismic waves, and it varies from 10 mm/sec to 100 mm/sec. Although our method of analysis is very simple, some features of waveforms closely relating to its activity mode can be found by superimposing the TRG seismograms.

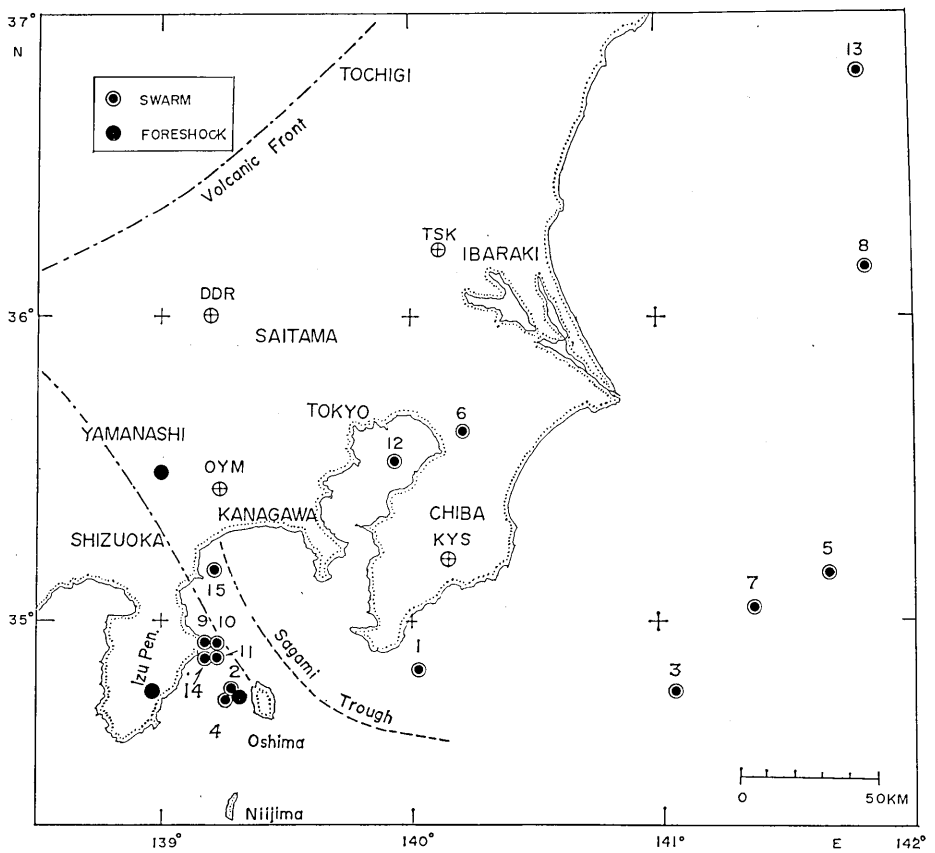

Fig. 4.2. Distribution of the epicentral areas of earthquake swarms and foreshocks. Numerals attached to double circles refer to the swarm number listed in Table 1. Solid circles show the foreshocks of the eastern Yamanashi Prefecture earthquake of 1976, the Kawazu earthquake, Izu Peninsula of 1976 and the Izu-Oshima-kinkai earthquake of 1978, respectively.

4.3. Waveform feature of earthquake swarms

Figure 4.2 shows the epicentral areas of earthquake swarm and foreshock activities. Numerals attached to double circles refer to the swarm number listed in Table 1, and the epicenters represented by solid circles refer to the foreshock activities of the 1976 eastern Yamanashi Prefecture earthquake, the 1976 Kawazu earthquake, Izu Peninsula and the 1978 Izu-Oshima-kinkai earthquake. The earthquake swarms are distributed over a wide area. In particular, it is noticed that the earthquake swarms and the foreshocks occurred in almost the same area near Oshima (Nos. 2 and 4). The waveform analyses of these sequences therefore will give us some useful information about the difference in nature between the two kinds of activities. The studies of individual sequences have been reported previously (TSUJIURA, 1977, 1978b, 1979a, 1979b, 1980, 1981), and here these studies will be summarized with some additional new data.

4.3a. Earthquake swarm off Kawanazaki, Izu Peninsula in 1978 (No. 9 in Table 1)

On November 24 of 1978, the swarm activity started in an area off Kawanazaki, Izu Peninsula, and this activity continued for about 20 days with repeated intermittent bursts of activity (TSUMURA *et al.*, 1979). During this earthquake swarm, 365 earthquakes with magnitudes between 1.5 and 3.0 were studied in terms of waveform analysis.

In the course of the examination of waveforms using triggered-seismograms we noticed that the earthquakes in a certain time interval (e.g., one hour) have similar waveforms. Figure 4.3 shows a comparison of seismograms obtained at Ohyama station (OYM) during an interval of about 16 minutes. High correlation between the corresponding traces is clearly seen, especially when events of similar size are compared. Moreover, the arrival times of S and later phases measured from the P-wave onset also agree within a range of 0.05 sec. We refer hereafter to these earthquakes with similar waveforms as a group of "similar earthquakes" or an "earthquake family" (HAMAGUCHI and HASEGAWA, 1975). However, the criterion of the earthquake family is somewhat uncertain. The earthquake family is defined here as a group of earthquakes whose seismograms show that the peaks and troughs of the P and S wave groups coincide with each other and that the S-P times fall within some limited ranges which depend on the earthquake size. The differences of S-P times used here are about 0.1 sec for $M=3$ and about 0.5 sec for $M=5$ earthquakes.

Figure 4.4 shows a comparison of seismograms at the Hokiyama station (HOK) for the same events as shown in Fig. 4.3. The HOK

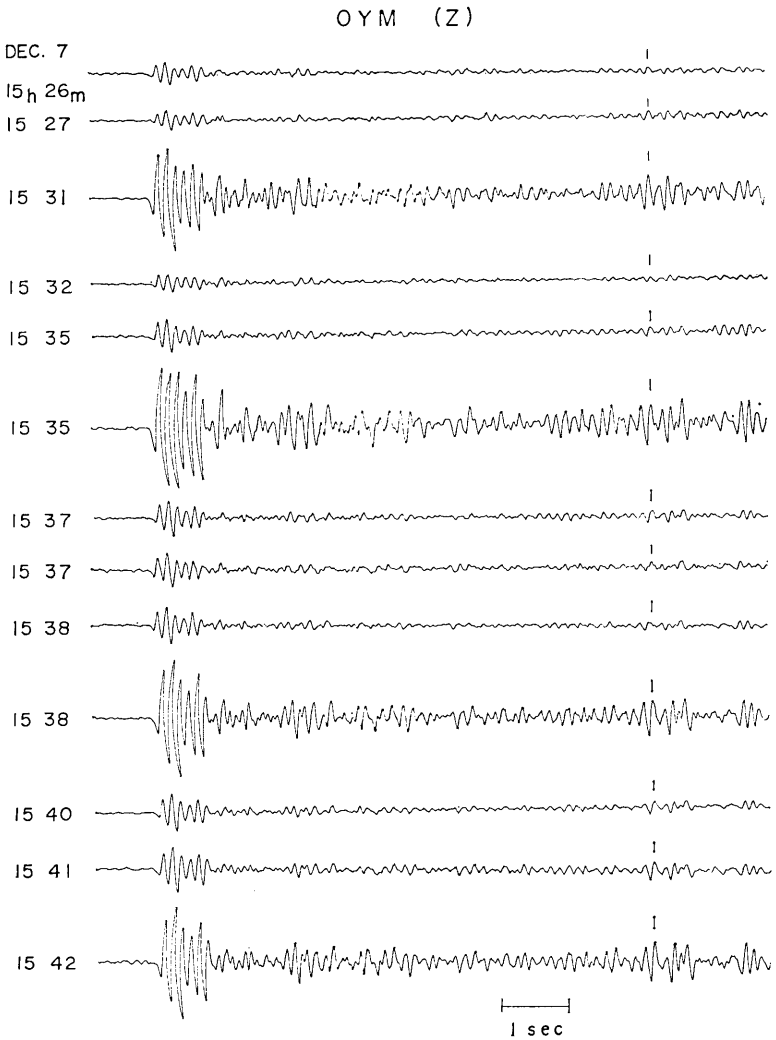

Fig. 4.3. Comparison of the seismograms with similar waveforms obtained by the vertical component (Z) at OYM during a 16 minute interval for the 1978 earthquake swarm off Kawanazaki, Izu Peninsula. Magnitudes of these events lie between 1.4 and 2.6.

station is located at a shorter epicentral distance ($\Delta \cong 10$ km) than the OYM station and in a different azimuth from the epicentral area (Fig. 4.2). As seen in Fig. 4.4, the seismograms at a shorter epicentral distance give more detailed similarities in the frequency range up to 10 Hz. It is noticeable that isolated wavelets, as indicated by dotted circles, are commonly observed even in the coda waves. Similar features, but with different waveforms, are seen for earthquakes in other periods of this sequence. Nineteen groups with their own waveform features are found for 264 earthquakes selected from the total

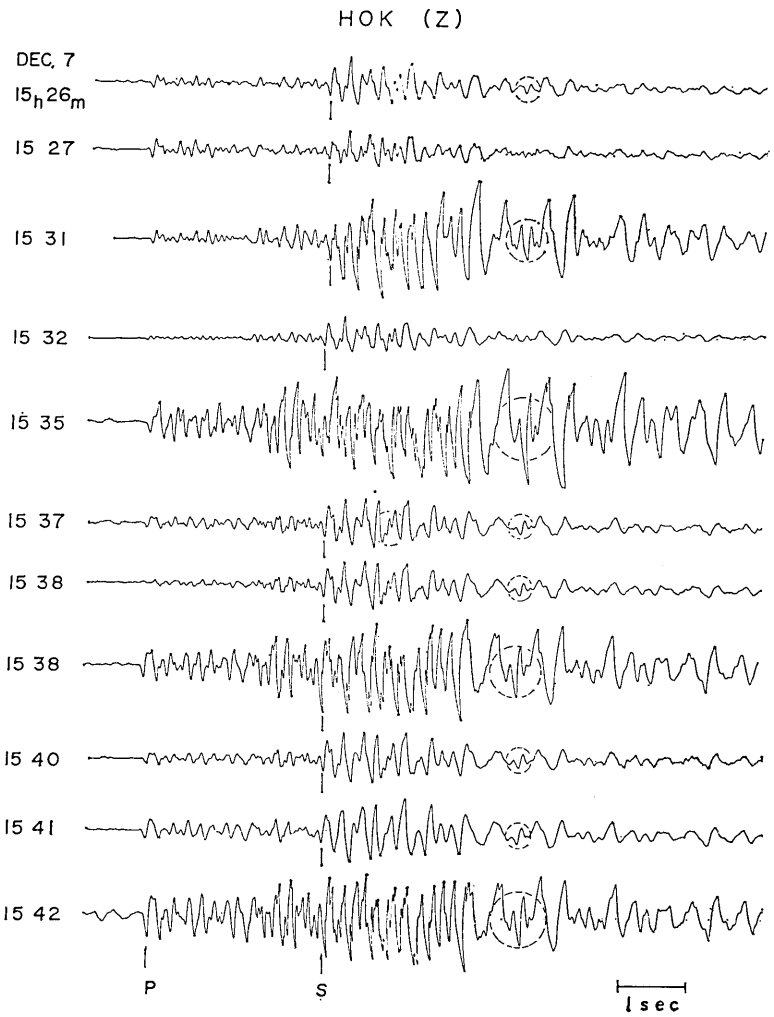

Fig. 4.4. Comparison of the seismograms obtained at HOK for the same earthquakes shown in Fig. 4.3. Note that isolated wavelets indicated by dotted circles are commonly observed even in the coda waves.

365 earthquakes (TSUJIURA, 1979a).

4.3b. Earthquake swarm in northern Tokyo Bay in 1979

The earthquake swarm which occurred in northern Tokyo Bay during the period from July 11 to August 3, 1979 was studied on the basis of the waveform analysis. This swarm activity was monitored by the magnetic-tape recording system consisting of six stations distributed around the swarm area. Thirty-four earthquakes with magnitudes between 1.0 and 3.0 were found in the monthly list of ERI. Among these earthquakes, sixteen with moderate-size amplitudes on magnetic tape were finally selected. The magnitudes of these events

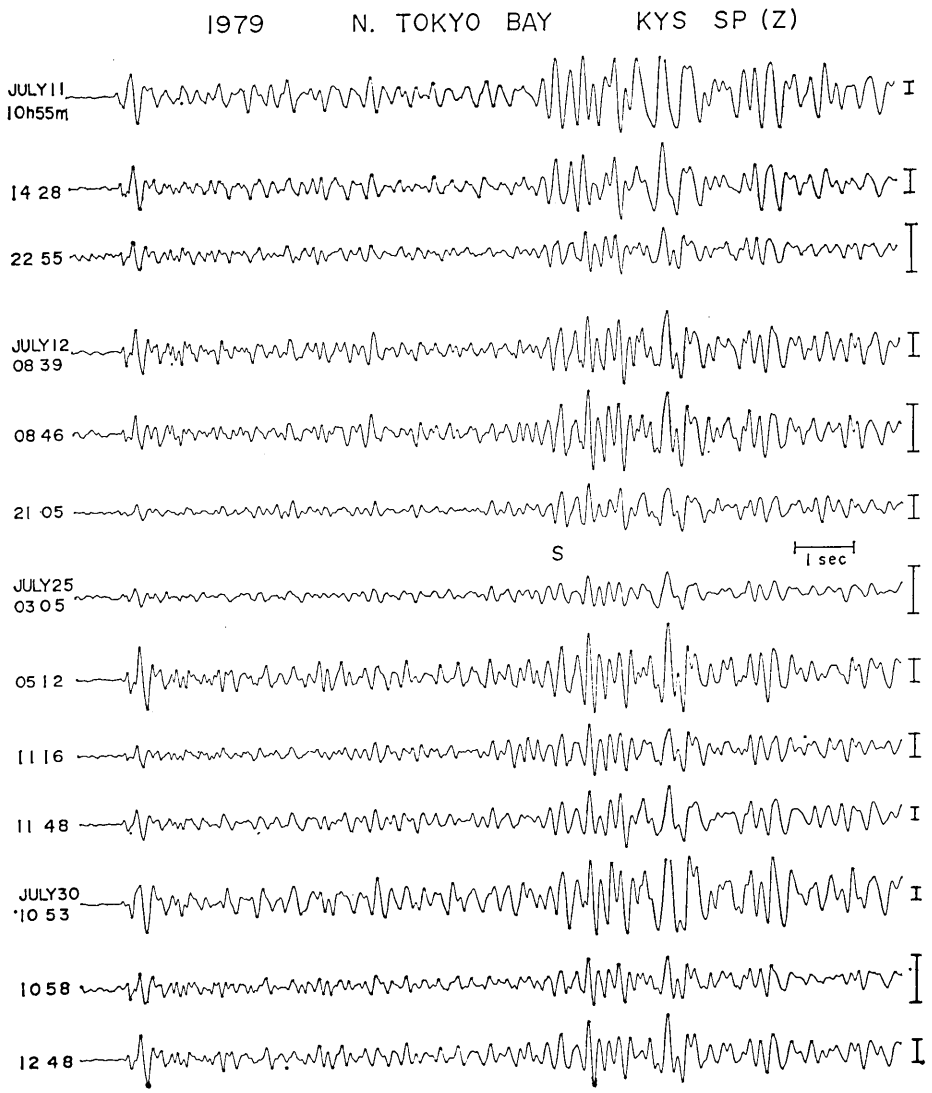

Fig. 4.5. Comparison of the seismograms obtained at KYS for the earthquake swarm in northern Tokyo Bay. The amplitude of each event is almost normalized by changing the gain of play-back amplifier from magnetic tape. Relative differences of the gain are shown at the end of each seismogram by error bars. Magnitudes of these events lie between 1.8 and 3.0.

range from 1.8 to 3.0.

Figure 4.5 shows a comparison of seismograms obtained by the vertical component seismograph (Z) at Kiyosumi station (KYS). The amplitude of each event is almost normalized by changing the gain of the play-back amplifier. The relative differences of the gain are shown at the end of the seismogram by error bars. Although the absolute

amplitudes are different by a factor of more than 10, similarities of waveforms are apparent over the entire record length, especially the peaks and troughs of the P and S-wave groups coincide through a sequence. Earthquakes with similar waveforms, of course, are expected to have similar S-P times. In fact, we find that the S-P times of these events do not differ by more than 0.06 sec. Similar results for the waveforms were obtained from the other five stations (TSUJIURA, 1980). Thus, it may be concluded that the swarm activity in northern Tokyo Bay also consisted of events with similar waveforms belonging to an earthquake family.

4.3c. Earthquake swarm off the east coast of the Izu Peninsula in 1980 (No. 14 in Table 1)

An earthquake swarm occurred in an area off the east coast of the Izu Peninsula during the period from June 24 to July 28, 1980. This swarm contained many bursts of activity usually lasting for about one hour. The swarm activity in this area occurred repeatedly

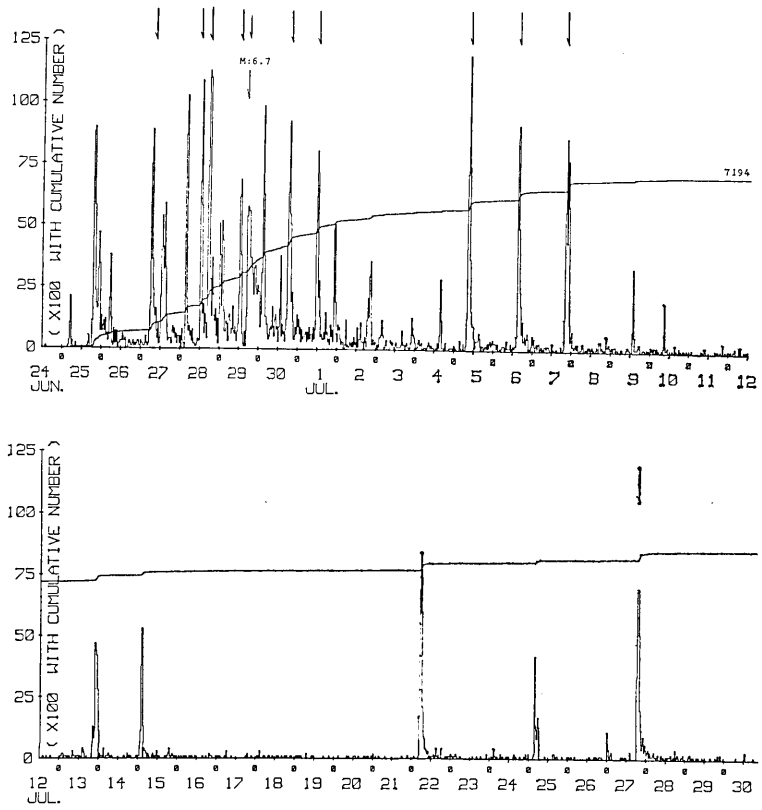

Fig. 4.6. Frequency distribution of earthquakes for every 30 minutes obtained at OYM for the 1980 earthquake swarm off the east coast of the Izu Peninsula (after ERI, 1981). The seismic activities indicated by arrows are used for the present study.

after 1978, and the present swarm shows the highest activity (e.g., KARAKAMA *et al.*, 1980).

Figure 4.6 shows the frequency distribution of earthquakes for every 30 minutes (ERI, 1981). We are especially interested in the activity mode during the most active stage of the swarm. Eleven sequences indicated by arrows in Fig. 4.6 were finally selected, and the waveform analysis was performed by superimposing the triggered-seismograms at five stations.

Figure 4.7 shows a comparison of seismograms obtained at the Hokiyama station (HOK) during an interval of about 15 minutes. The similarity of waveforms is clearly demonstrated from the *P*-wave onset

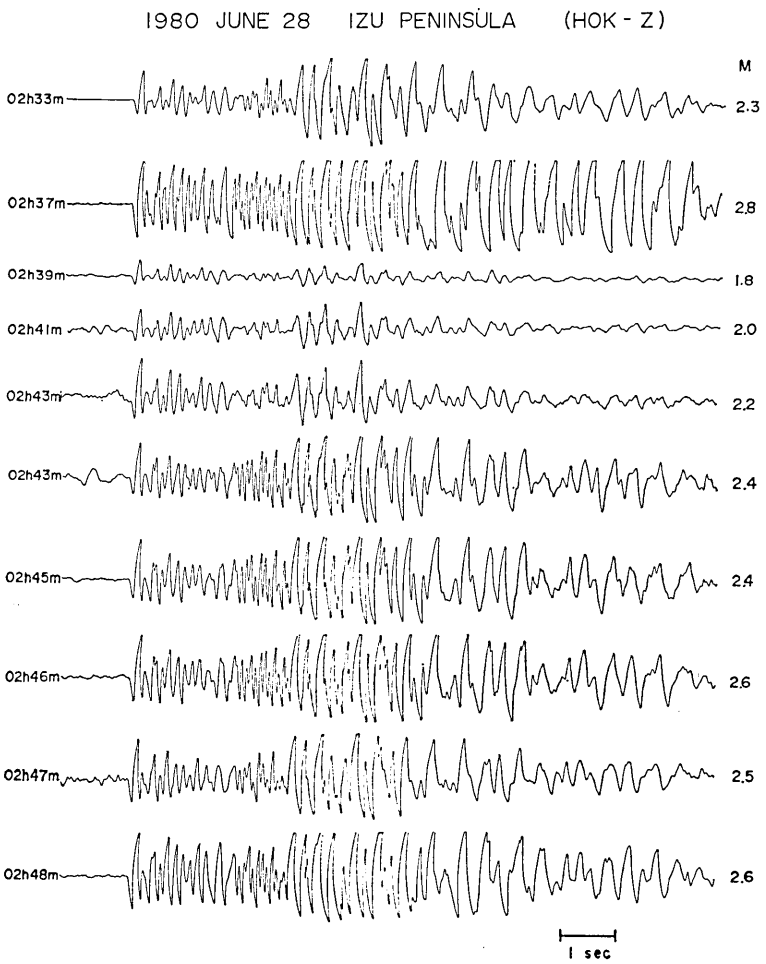

Fig. 4.7. Comparison of the seismograms obtained by the vertical component (Z) at HOK during a period of 15 minutes. Magnitudes of these events lie between 1.8 and 2.8. Note that high correlation of corresponding waves between the seismograms.

till coda waves. Similar waveform features can be seen also for the seismograms of the other four stations (TSUJIURA, 1981).

The time interval between two successive earthquake families depends on the degree of seismic activity. When the activity is high, the time interval is short, and another family appears soon after the activity of the initial family is finished. Figure 4.8 shows an example of the distribution of earthquake families during a 70-minute interval of concentrated activity. The amplitude of each event shows the relative amplitude of S waves on the 3 Hz-band taken from the filtered-seismograms at DDR and TSK, and the scale of the ordinate on the right-hand side indicates the magnitude (M) which was determined at DDR by the F-P time method (HORI, 1973). Solid and dashed lines represent the upward and downward initial motion at HOK, respectively. Numerals at the top show the group number of the earthquake family. We find that during a certain active period several earthquake families with different source mechanism appear alternately.

The S-P times for events in each family do not differ by more than about 0.06 sec, and the S-P times for events in the different families may differ within a range of about 0.2 sec (TSUJIURA, 1981). Such behavior suggests that the earthquakes in the active period do not occur randomly in space and that they occurred only within several limited small areas.

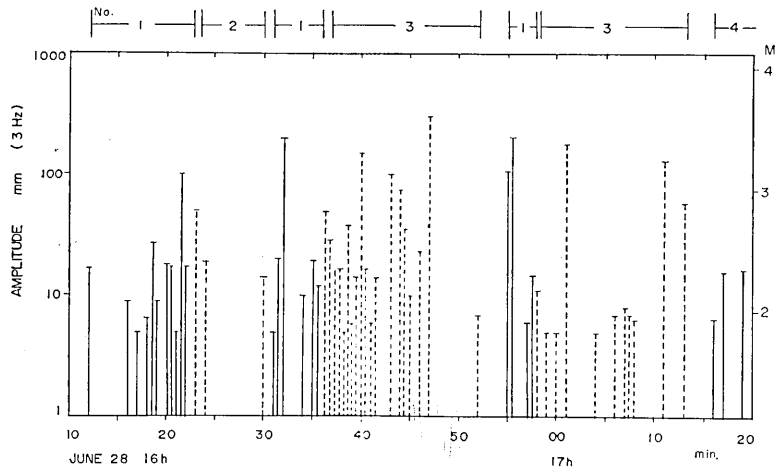

Fig. 4.8. Distribution of earthquake families obtained for a swarm sequence of about a 70-minute period of concentrated activity. Numerals in the upper abscissa show the group number of earthquake families. Solid and dashed lines show the upward and downward initial motions at HOK, respectively. The amplitude and magnitude (M) are determined on the basis of the filtered-seismograms at DDR and TSK and from the F-P time at DDR.

Figure 4.9 shows the temporal distribution of earthquake families in another period of this series. An alternate occurrence of four families is apparent the same as those shown in Fig. 4.8. Two large earthquakes with $M \geqq 4.5$ occurred in this sequence. The source depths for these events are about 10 km (KARAKAMA *et al.*, 1980). Such events are usually followed by aftershocks. In the present case, however, the activity preceding the M4.5 earthquake is higher than the activity following the event. This is probably one of the most important features in the activity of similar earthquakes. This feature can be qualitatively explained as follows. The earthquakes belonging to a family occur on the same fault plane as a repeated slipping or a repeated incomplete rupture, and the largest event occurs as the earthquake with maximum slip or complete rupture corresponding to the "highest stress drop earthquake" (AKI *et al.*, 1977). Consequently, only a weak activity will be followed on the same fault plane. On the other hand, this maximum stress release produces the stress concentration elsewhere and promotes the occurrence of another family.

Similar analyses were performed for 10 sequences, each of which has an activity of one hour, and it confirmed that they have similar activity modes (TSUJIURA, 1981). Table 3 shows the proportion of earthquake occurrences in families together with the number of families

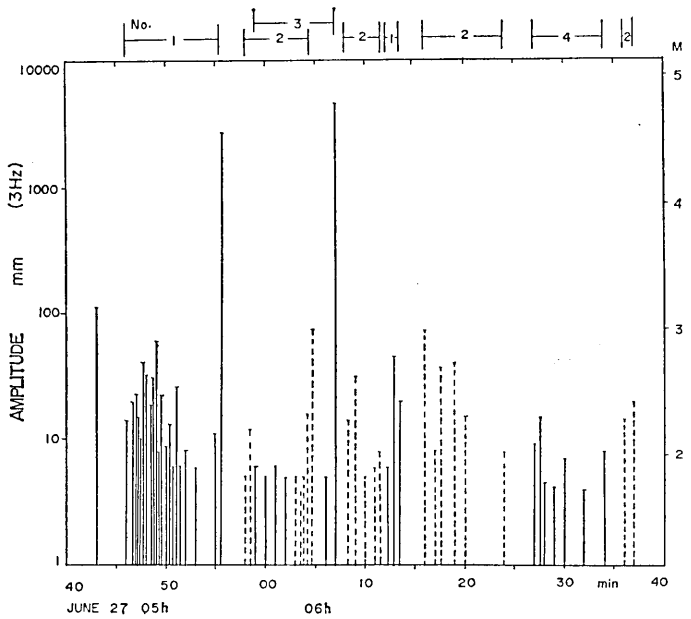

Fig. 4.9. Temporal distribution of the earthquake families including large events with $M \geqq 4.5$. Note that the activity preceding the large event is more dominant than the activity following the event. Explanation of the other symbols is the same as those for Fig. 4.8.

Table 3. Ratio of the number of earthquakes belonging to earthquake families to the total number of earthquakes. N; total number of earthquakes, n; number of earthquakes in the family, F; number of earthquake families, M_{max}; magnitude of the largest earthquake in each sequence.

Date	Time				N	n	n/N	F	M_{max}
	h	m	h	m			%		
June 27	05	43	— 06	37	77	65	84	4	4.9
June 28	11	25	— 12	20	80	66	83	4	4.9
June 28	16	12	— 17	19	87	70	80	4	3.8
June 29	12	07	— 13	12	44	35	80	4	3.2
June 30	17	20	— 18	15	56	41	73	5	3.6
July 1	10	45	— 11	40	50	40	80	5	3.4
July 5	07	45	— 09	02	51	38	75	6	3.3
July 6	13	58	— 14	58	77	61	79	4	4.1
July 7	19	43	— 20	57	42	34	81	4	4.5
July 27	17	49	— 18	50	53	35	66	4	4.6

recognized. It can be seen that about 80 per cent of earthquakes belong to several families.

Besides the earthquake groups described above, the activity associated with an extremely large earthquake of $M=6.7$ (see Fig. 4.6) is quite different from those of the other 10 sequences. The $M6.7$ earthquake appeared suddenly without any preceding small earthquake and was followed by many small earthquakes. This suggests the activity of the main shock-aftershock type. The activity mode for 41 earthquakes which occurred during the three hour period following the $M6.7$ shock was studied by the same procedure. All of these events appear with an individual waveform character except for two events with similar waveforms (TSUJIURA, 1981).

4.3d. Other earthquake swarms

Similar analyses of waveform were extended for the other swarm activities listed in Table 1, and it confirmed that the swarm activity in a certain time interval consisted mainly of events with similar waveforms (TSUJIURA, 1979b). Similar features of waveforms can be seen for many earthquakes of the swarm sequences in different regions (STAUDER and RYALL, 1967; SATO *et al.*, 1979; TSUKUDA, 1980; OKADA *et al.*, 1981).

Most of earthquakes studied above, however, were earthquakes with magnitudes between 1.5 and 4. When the magnitude of an earthquake increases, the similarity in high-frequency components becomes somewhat uncertain. Figure 4.10 shows a comparison of seismograms with magnitudes of 4.8 and 6.1 obtained by the MP seismograph at TSK for the 1978 earthquake swarm east off Chiba Prefecture (No. 7 in Table 1). The upper two seismograms show the

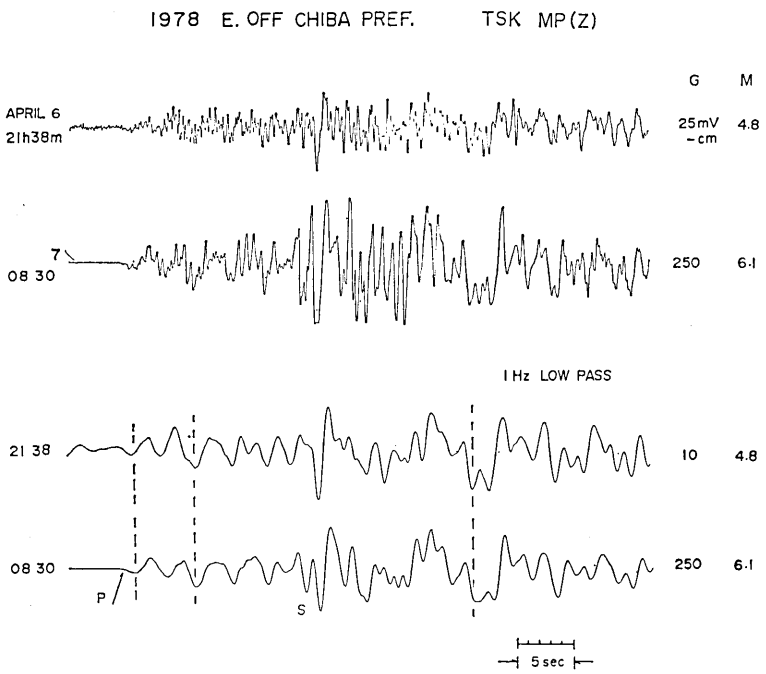

Fig. 4.10. Comparison of the seismograms with magnitudes of 4.8 and 6.1 obtained by the MP seismograph at TSK for the 1978 earthquake swarm east off Chiba Prefecture. The upper two show the original seismograms and the lower two show the seismograms passing through the low-pass filter with cut-off frequency of 1 Hz. G; relative differences of the gain of play-back amplifier. Similar waveforms and S-P times are seen in low-frequency seismograms.

original and lower two show the seismograms passing through the low-pass filter with a cut-off frequency of 1 Hz. Although the high-frequency components ($f>2$ Hz) do not coincide with each other (upper seismograms), the low-frequency components ($f<1$ Hz) agree well in waveforms and S-P times.

On the other hand, recent observations of small swarms in the near-field (S-$P \cong 1$ sec) provide the data with more detailed similarities of waveforms and S-P times. Figure 4.11 shows seismograms of an earthquake family in the western part of Tochigi Prefecture obtained by the SP seismographs with high (H) and (L) magnifications at Uchino-komori near Ashio (UKM). The magnitudes of these events lie between -1.0 and 1.0. The similarity of waveforms and the equality of S-P times (Δt_{S-P}) are clearly demonstrated in the frequency range up to 30 Hz and in the distribution of S-P times less than 0.008 sec. Therefore, the frequency range with similar waveforms is a function of the earthquake size. Roughly speaking, the lower limits of frequency with similar waveforms are about 0.5 Hz for $M=6$, about 6

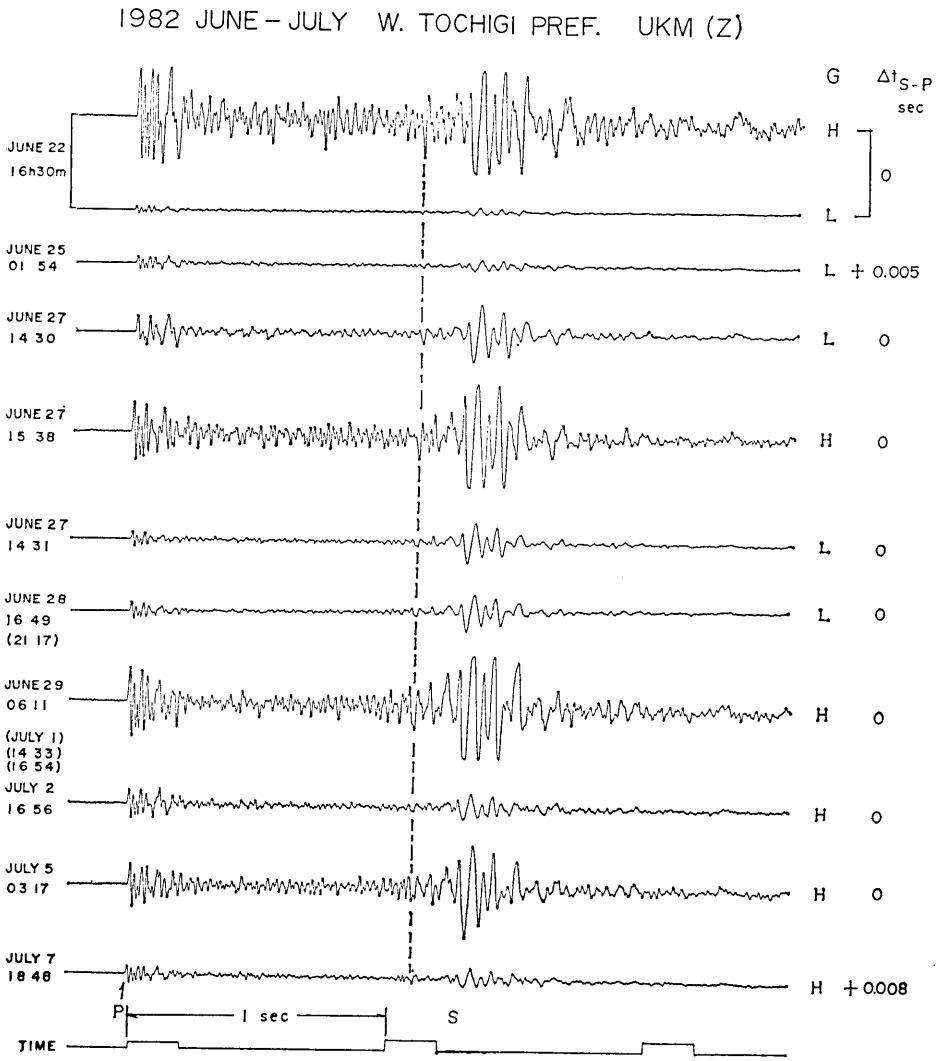

Fig. 4.11. Comparison of the seismograms obtained by the SP seismographs with high (H) and low (L) magnifications at UKM for the earthquake swarm in the western part of Tochigi Prefecture. The difference of magnifications between high and low gain seismographs is twentyfold. The magnitudes of these events lie between −1.0 and 1.0. The similarity of waveforms and the equality of *S-P* times are seen in the frequency range up to 30 Hz and in the distribution of *S-P* times less than 0.008 sec.

Hz for $M=3$ and about 30 Hz for $M=1$ earthquakes, respectively. These values seem to relate to the source time function of their earthquakes as will be discussed later. Thus, it may be concluded that the earthquakes in a given swarm sequence consist mainly of events with similar waveforms belonging to one or more families, though their frequencies depend on the earthquake size.

4.4. Spatial distribution of swarm earthquakes

In view of the observed time difference of S-P at our stations, the epicentral area for the swarm sequence determined by the conventional method may be too large (TSUJIURA, 1979a, 1980). In order to obtain the precise location of epicenters, detailed measurements of S-P times at each station were made for a given swarm sequence. We shall deal here with the earthquake swarm in northern Tokyo Bay (No. 12 in Table 1). Tokyo Bay is located in the middle of our seismic network, and precise locations of these events are expected.

As shown previously (Fig. 4.5), the seismograms of this swarm sequence showed similar waveforms. Figure 4.12 shows examples of the superimposition of seismograms obtained at KYS and DDR for this swarm sequence. The paper speed was set at 50 mm/sec. The peaks and troughs for the P and S waves closely coincide with the seismograms at each station. Small differences of S-P times therefore can be obtained from the time difference of the P-wave group when the seismograms of S waves are fixed to agree with each other.

Table 4 shows the distribution of the relative differences of S-P time obtained through the swarm sequence. It can be seen that the deviation of S-P times falls within a range of 0.05 sec, indicating systematic differences at each station.

Figure 4.13 shows the relative location of epicenters against the reference earthquake (14 h 28 m, July 11) determined by using the data listed in Table 4 and by assuming a value of Ōmori constant $k=8$ km/sec. Numerals attached to the solid circles correspond to the event number in Table 4. The epicenter with a cross mark shows the reference earthquake (No. 2), and the epicenters inside dotted circles

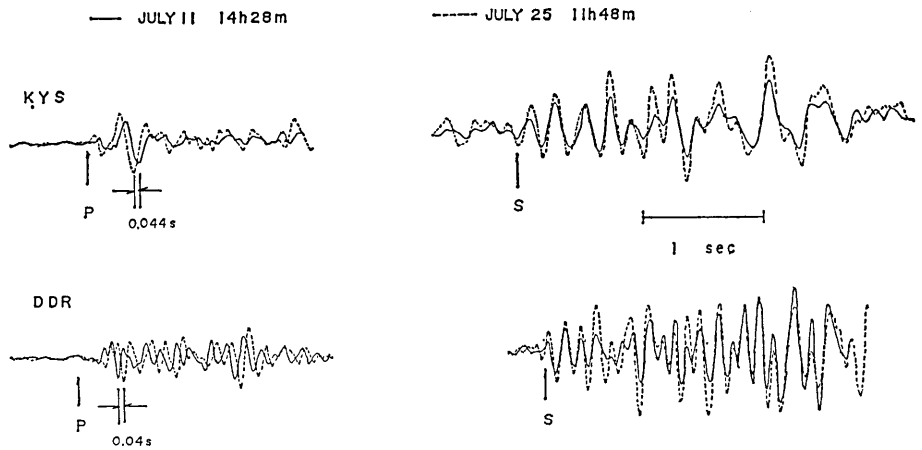

Fig. 4.12. Superimposition of the seismograms for two earthquakes obtained at KYS and DDR. Note the small differences of S-P times (<0.044 sec).

Table 4. Distribution of the relative differences of S-P times (Δt_{S-P}) against the reference earthquake (No. 2). The origin time and magnitude (M) are taken from the monthly list of ERI, and the M_J is taken from the list of earthquakes by the JMA.

No.	Date	Time	M	M_J	Δt_{S-P} sec				
		h m s			KYS	DDR	TSK	TAK	OYM
1	July 11	10 55 54.4	2.7	2.9	0.008	−0.01	0	0.01	0
2		14 28 45.1	2.4	—	0	0	0	0	0
3		22 55 15.3	1.8	—	0.01	−0.012	−0.024	0.016	0
4	July 12	08 39 11.3	2.0	—	0.012	−0.02	−0.024	0.024	−0.01
5		08 46 39.0	1.9	—	0.012	−0.02	−0.02	0.02	−0.01
6		20 20 01.6	2.1	—	0.036	−0.03	−0.024	0.024	−0.014
7		21 05 03.0	1.8	—	0.036	−0.032	−0.028	0.02	−0.014
8	July 16	17 55 11.6	2.0	—	−0.01	0.008	—	—	—
9	July 25	03 05 08.6	1.8	—	−0.04	—	−0.04	—	—
10		05 12 28.1	2.6	2.8	−0.01	0.016	−0.01	0.018	0.018
11		11 16 23.9	2.2	2.5	0.044	−0.04	−0.04	0.03	−0.01
12		11 48 10.7	2.9	3.0	0.044	−0.04	−0.044	0.034	−0.01
13	July 30	10 53 51.0	3.0	3.3	0.05	—	−0.046	0.028	0.014
14		10 58 44.1	2.1	—	0	—	−0.01	0.018	0.018
15		12 48 28.7	2.4	2.7	0	—	−0.01	0.016	0.016
16	Aug. 3	08 58 39.7	2.2	—	0	0.02	−0.038	0.044	0.044

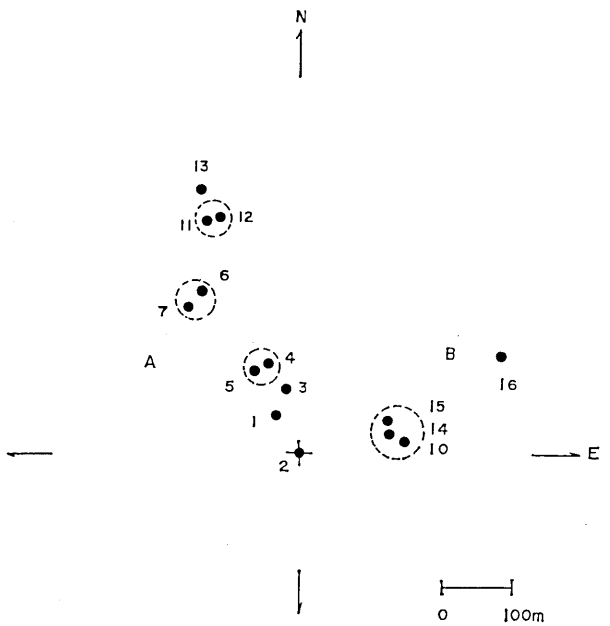

Fig. 4.13. Relative epicentral locations for the reference earthquake (No. 2). Numerals attached to the circles correspond to the event number shown in Table 4.

show the events with S-P times closer than 0.01 sec, indicating an exact agreement of waveforms at five stations (see Fig. 6 in TSUJIURA, 1980). Two earthquakes, numbers 8 and 9, are not included in this figure due to a poor signal-to-noise ratio.

As seen in Fig. 4.13, the epicenters are divided into two groups, one consisting of events with a linear trend (A), and the other consisting of events concentrated in a small area (B). Although our epicenter determination has an error of about 50 meters, the pattern of epicenters for the sequence exhibits some interesting features. For example, the earthquake occurs first in the southeast end of this series and its activity migrates mainly to the northwest with a length of about 400 meters, terminated by event No. 13. After that, the activity returns to the initial focal area (group B). Considering the similarity of waveforms and the linear arrangement of epicenters, it is most likely that the events belonging to group A occurred along the same fault plane slipping repeatedly. In particular, as inferred from the close agreements of waveforms and S-P times at five stations, the events inside the dotted circles must have occurred on the same fault plane in the manner of a "stick-slip" observed in the laboratory experiments on rocks (e.g., BRACE, 1972).

Our observation can be understood also with the aid of the earthquake model called the "barrier model" proposed by DAS and AKI (1977). The migration of earthquake clusters from A to B may be due to successive stress concentrations at barriers distributed on the fault as slipping proceeds from A to B.

As mentioned in the preceding sections, small deviations of S-P times were observed for the earthquake families in different regions. A tight cluster of epicenters distributed within an area of 300-1000 meters was found also in the earthquake families of the Usu volcano earthquake swarm (WANO and OKADA, 1980; OKADA *et al.*, 1981) and in the ordinary swarm activity (TSUKUDA, 1980). Thus, it may be concluded that the events of an earthquake family occur within a very small focal area probably on the same fault plane. The observation of numerous families with their own waveform characteristics in a given swarm sequence then suggests the existence of numerous cracks and faults bounded by barriers. This evidence is consistent with the study of MOGI (1963b) which concluded that the earthquake swarm occurs in a heterogeneous region.

Another feature indicating the nature of an earthquake swarm is that the largest earthquake in a given family usually occurs in the late stage of its sequence. As an example, Figure 4.14 shows the temporal distribution of earthquakes with $M > 3.5$ taken from the monthly lists of JMA for the 1978 earthquake swarm east off Chiba

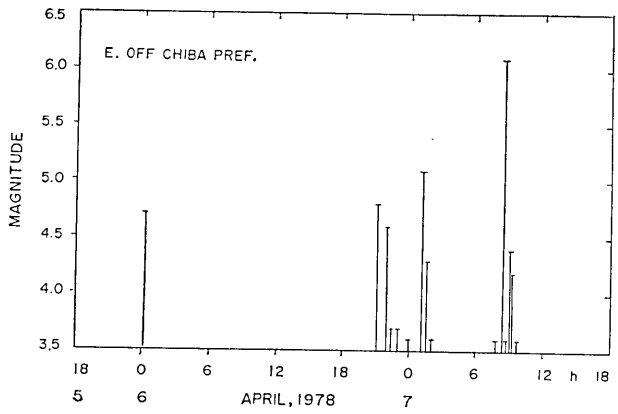

Fig. 4.14. Temporal distribution of earthquakes with $M>3.5$ for the earthquake swarm east off Chiba Prefecture.

Prefecture (No. 7 in Table 1). According to our criterion of an earthquake family, this swarm corresponds to one earthquake family (Fig. 4.10). The largest earthquake with $M=6.1$ occurred about 32 hours after the swarm started, and it is also noticed that the activity preceding the $M6.1$ earthquake was higher than the activity following the event. Such behavior is consistent with the 1980 earthquake swarm on the Izu Peninsula as was previously mentioned (TSUJIURA, 1981).

4.5. Conclusion

Through the waveform analysis of earthquake swarms, salient features of the waveforms of their earthquakes were found. The main features are as follow:

(1) The earthquakes in a swarm sequence are concentrated within a short time interval.

(2) The swarm activity in a certain time interval (e.g., one hour) mainly consists of events with similar waveforms belonging to the so called "earthquake family" (70-80%).

(3) The epicenters of an earthquake family are distributed in a tight cluster, within an area of a few hundred meters ($M_{\max}\cong 3$).

(4) When the activity is high, numerous families with their own waveform characteristics are observed during a swarm sequence.

(5) The largest earthquake in a given family usually occurs in the late stage of its sequence.

From the viewpoints of the similarity of waveform and the spatial distribution of epicenters, it may be concluded that the events belonging to earthquake family occur on the same fault plane as a repeated slipping or an incomplete rupture. The existence of numerous families

in a given swarm sequence then suggests that there exists numerous cracks and faults bounded by barriers.

CHAPTER 5

Spectral Analysis of Earthquake Swarms

5.1. Introduction

In the preceding chapter we pointed out that the seismic activity in a swarm sequence consists mainly of events with similar waveforms belonging to one or more earthquake families (70-80%). The time duration of the occurrence of an earthquake family depends on the degree of seismic activity. When the activity is high, numerous families with their own waveform features are observed during the swarm sequence. On the other hand, for a weak activity, such as the 1979 earthquake swarm in northern Tokyo Bay, the earthquake family continued for about one month with repeated intermittent activity (TSUJIURA, 1980). Therefore, the earthquake family is the basic unit in an earthquake swarm.

As was pointed out by MOGI (1963b), the earthquake swarm usually does not contain an extremely large earthquake. In fact, in the Matsushiro earthquake swarm, 56 earthquakes with magnitudes between 4.5 and 5.1 were observed, but no earthquakes were found with magnitudes above 5.2 (HAGIWARA and IWATA, 1968). Similar tendencies, but limited to a magnitude about 4, were seen in the swarm activity of Hokkaido (MOTOYA *et al.*, 1979) and in the earthquake swarm of Usu volcano (OKADA *et al.*, 1981). As mentioned in the preceding chapters, however, the largest earthquake contained in each earthquake swarm differs in magnitude from 3.2 to 6.7. Moreover, the frequency-magnitude relationship in an earthquake family shows a remarkable peak or flat portion which differs from that of an ordinary seismic activity (WANO and OKADA, 1980; OKADA *et al.*, 1981). We shall first study spectral features of the earthquake families, and in a later section the growth of the source spectrum with magnitude will be studied in the form of the scaling law proposed by AKI (1967). These results will be useful for a better understanding of the nature of earthquake swarms.

5.2. Method of analysis

In order to obtain the source spectrum of earthquake swarms the spectral analysis is made for S waves using the data of filtered-seismograms described in Chapter 2. The method of analysis is the same as that of our previous studies (TSUJIURA, 1977, 1978b). The maximum

amplitudes (peak-to-peak) for S waves are measured directly on the 6-band filtered-traces, and the relation between the amplitudes and their frequencies is studied. Although our method of the analysis is a rough estimation, it is useful when a great deal of data are processed.

5.3. Spectral feature of earthquake swarms

As shown in the previous sections, the earthquake family was a basic unit in swarm earthquakes. Fig. 5.1 shows the filtered-seismograms belonging to one earthquake family obtained at OYM during a period of about seven minutes for the earthquake swarm on the northern Izu Peninsula (No. 11 in Table 1). The frequency on the left-hand side (f_0) shows the center frequency of each band-pass filter. They show similar spectra independent of the absolute value of amplitudes. Such a feature of the spectrum is more clearly seen if we plot the amplitude at one frequency as a function of the amplitude at another.

Figure 5.2 shows the spectral amplitudes of S waves at 6 and 12 Hz versus 3Hz for the events belonging to one earthquake family. Each plot represents an earthquake as derived directly from filtered-seismograms. In order to obtain a wide dynamic range of the spectrum, the data from DDR equipped with the same system may be used. Solid circles with cross mark show the common earthquake for both stations. From the combined data at two stations the relative growth of the

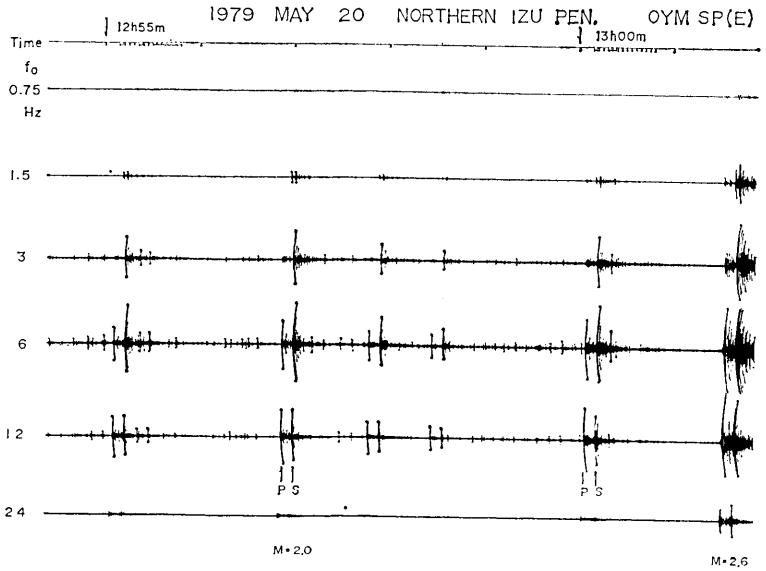

Fig. 5.1. Examples of the filtered-seismograms. f_0 shows the center frequency of band-pass filter with one octave bandwidth (see Fig. 3.5). Tick marks at the top are minute marks.

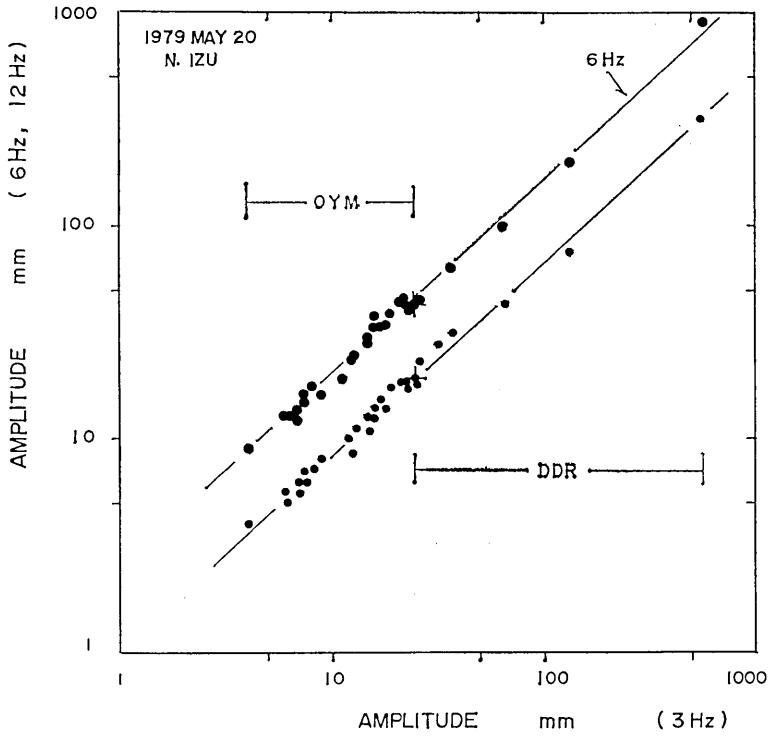

Fig. 5.2. Relation between the *S*-wave amplitudes at 6 and 12 Hz and the *S*-wave amplitude at 3 Hz for the events belonging to one earthquake family. The rates of increase of spectral amplitudes obtained from two stations are the same at various frequencies. The solid circle with cross mark shows the common earthquake for both stations.

spectrum with magnitude is obtained for a wide dynamic range. Magnitudes of these events range from 1.5 to 3.5. The conformity of the straight lines to the data implies that the spectral shape of these earthquakes does not change with magnitude in the frequency range between 3 and 12 Hz.

Another example of the growth of spectra with magnitude is shown in Fig. 5.3. These earthquakes were obtained from the same swarm sequence but in a different period (March in 1979). Except for the amplitude of the 12 Hz band for two events with large amplitude, similar trends of the growth of amplitudes are again obtained. We now examine the growth of spectral amplitudes in the form of the scaling law of earthquake source spectrum.

5.4. Scaling law of source spectrum

Consider a point dislocation source with the seismic moment time function $M(t)$ we denote its Fourier transform by $M(\omega)$. The Fourier

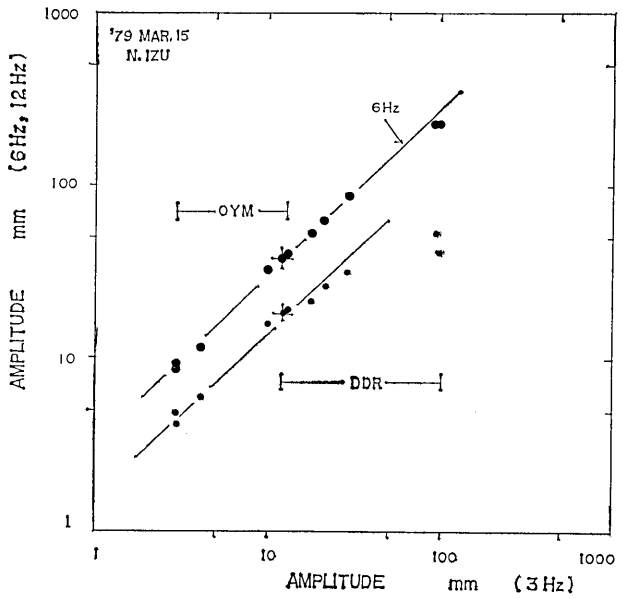

Fig. 5.3. Relation between the *S*-wave amplitudes at 6 and 12 Hz and the *S*-wave amplitude at 3 Hz for the events belonging to one earthquake family. The rates of increase of spectral amplitudes are the same at various frequencies for small events, but the rate of increase for large events (M=2.5) becomes smaller for the spectral amplitude at 12 Hz than for one at 3 Hz.

transform $F(\omega)$ of far-field displacement due to S waves at a distance r from the source can be given by the following (BRUNE, 1970)

$$|F(\omega)|=c(4\pi\rho\beta^3 r)^{-1}|\dot{M}(\omega)| \tag{5.1}$$

where c is a geometrical spreading factor, ρ is the density, β is the shear-wave velocity and $\dot{M}(\omega)$ is the Fourier transform of the time derivative of seismic moment.

If the *S*-wave signal has an impulsive form of duration shorter than the filter time constant, we can approximately relate the amplitude As measured in the filter trace with the Fourier transform $F(\omega)$ as (AKI and CHOUET, 1975)

$$As=2\Delta f|F(\omega)| \tag{5.2}$$

where Δf is the bandwidth of the filter. From the known bandwidth of band-pass filter and the maximum amplitude of S waves measured on each filtered trace, the approximate spectral density can be estimated.

In order to obtain the source spectrum, the effect of the propagation path, such as the attenuation, must be taken into account to the observed spectrum. The attenuation of seismic waves is given by an exponential term of $\exp(\pi f r/QV)$, where f is the frequency, r is the

length of the path, V is the velocity and Q is the quality factor of attenuation.

Values of Q for body waves in the crust and uppermost mantle have been estimated for various seismic regions. Values of Q_α of 100-1000 have been obtained depending on the tectonic nature of the regions (PRESS, 1964; SUMNER, 1967; CLOWES and KAWASEWICH, 1970; O'NEILL and HEALY, 1973) and Q_β of 100-200 for the uppermost crust (KURITA, 1975; BAKUN and BUFE, 1975).

The Kanto district is located in the tectonically complicated region because of the existence of two subducting slabs, the Pacific plate and the Philippine Sea plate. The attenuation property as well as the source spectrum in this area also show a complicated pattern (TSUJIURA, 1973a). However, a systematic investigation for obtaining the Q value has not yet been made. Only a few attempts to obtain Q values were made by using the data of amplitude ratios of different frequency bands of body waves and their travel times (TSUJIURA, 1966, 1978a) and by using the spectral ratios of S and coda waves (AKI, 1980a, 1980b; SATO and MATSUMURA, 1980).

Our estimation of Q_β shows the values of 1200 for the area of TSK-A, 600 for TSK-B, 500 for DDR-A and 400 for DDR-B area, respectively. The area of A and B corresponds to northern and southern Kanto district bounded by the 36°N line (TSUJIURA, 1978a). These values of Q_β are somewhat larger value than those of other regions. Seismic waves traveling from earthquakes in the area of A to TSK pass through an inclined seismic zone (TSUJIURA, 1972). BARAZANGI and ISACKS (1971) suggested that the average Q_β in the inclined seismic zone of the Tonga region is on the order of 10^3. Moreover, the Q structure estimated in the interpretation of coda waves observed at the TSK-A area includes a low-Q zone (around 200) in the shallower crust and a high-Q zone (around 2500) in the deeper lithosphere (TSUJIURA, 1978a). Thus, the above large Q_β of 1200 is not unreasonable as an average over the depth range from 0 to 70 km. The estimation of Q_β for the other stations therefore can be made by the differnce of spectral ratios of the same earthquakes observed at TSK and DDR.

The site effect of the station due to the difference of local geology is another important factor in the correction. In obtaining the site factor, we used the spectral amplitudes as a function of the lapse time measured from the origin time. The TSK station is located on granitic rock, and there is no significant site effects. The site factors for five stations located on different formations were obtained from the comparison of spectral amplitudes of coda waves in the same lapse times basis on TSK (TSUJIURA, 1978a). However, these values seem to be too large for the site effect of S waves because the coda waves

are the back-scattering waves caused by the heterogeneities distributed randomly in space (AKI, 1969; AKI and CHOUET, 1975). About a half value of the site factors determined from coda excitation may be reasonable as the site effect of S waves. This is because estimated source spectra using these values produce fairly flat response at low frequencies and decay with frequencies roughly proportional to ω^{-2} beyond the corner frequency (TSUJIURA, 1978b). Using the method mentioned above, we obtained the source spectra for all swarm sequences shown in Table 1.

5.4a. Earthquake swarm off Kawanazaki, Izu Peninsula in 1978

The earthquake swarm which occurred off Kawanazaki, Izu Peninsula during the period from November 24 to December 10, 1978 was studied on the basis of the spectral analysis. As mentioned in Chapter 4.3a, this earthquake swarm mainly consisted of events belonging to 19 families. The source spectra of S waves for 264 events belonging to 19 families were obtained. Figure 5.4 shows the source

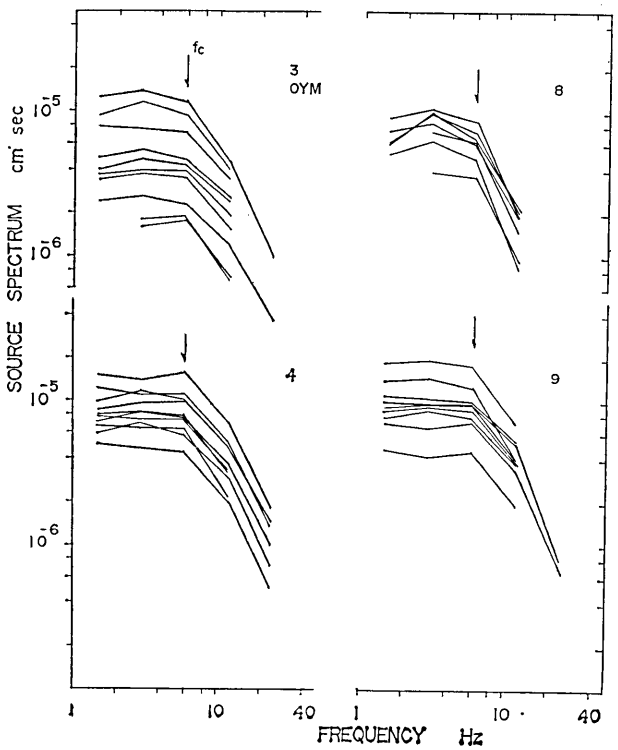

Fig. 5.4. Source spectra obtained from S waves at OYM for the events belonging to earthquake families, corrected for the attenuation with $Q_\beta=300$ and for the site factor. Arrows show the corner frequency (f_c). Numerals attached to each group of the spectrum show the index number of the earthquake family (see Table 1 in TSUJIURA, 1979a).

spectra for four selected earthquake families obtained at OYM, assuming the values of $Q_\beta = 300$, shear-wave velocity of 3.5 km/sec and the site correction dividing the observed spectra by 2 for $f \leqq 3$ Hz.

The long-period spectral level (Ω_0) and the corner frequency (f_c) are determined by fitting the spectra in two straight lines that intersect at the corner frequency. The approximate corner frequencies are indicated by arrows. It is noted that the corner frequency in a given family is kept constant at about 6 Hz, independent of the absolute value of amplitudes. Figure 5.5 shows the source spectra of other groups. Although the corner frequencies of events in two groups of No. 15 and No. 20 are slightly lower than the former groups (Fig. 5.4), again the corner frequencies agree well within the group.

In order to obtain the source spectra for a wide dynamic range the data from DDR equipped with the same system may be used. From the combined data from two stations the source spectra for the earthquakes differing in magnitude by about 1.5 units are obtained.

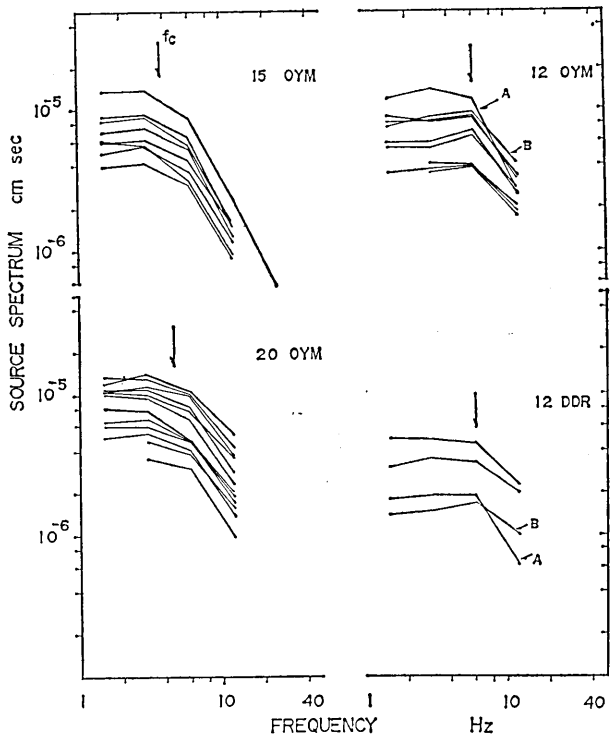

Fig. 5.5. Source spectra obtained from S waves at OYM and DDR for the earthquake families. Spectra indicated by A and B show the common earthquakes for both stations. Explanation of the other symbols is the same as those for Fig. 5.4. The corner frequency in each family is almost the same, but its value differs slightly among the families.

They show nearly the same corner frequency as shown in Fig. 5.5.

From each flat low frequency level (Ω_0), the corresponding seismic moment (M_0) is estimated by using Brune's formula

$$M_0=\frac{1}{c}4\pi\rho\beta^3 r\Omega_0 \tag{5.3}$$

where c is a geometrical factor, ρ is the density, β is the shear-wave velocity and r is the hypocentral distance. The estimated seismic moment by assuming $\beta=3.5$ km/sec, $\rho=2.8/\text{cm}^3$ and $c=0.8$ (THATCHER and HANKS, 1973) shows the values of 1×10^{19} dyne cm for $M=1.5$ and 3.5×10^{20} dyne cm for $M=3$ earthquakes, respectively.

According to MADARIAGA (1976) for a circular crack model, the corner frequency (f_c) for S wave spectrum is related to the fault radius (a) by

$$a=0.21\beta/f_c \tag{5.4}$$

where β is the shear-wave velocity. The estimated fault radii by assuming $\beta=3.5$ km/sec show the values of 120 and 200 meters depending on the event group.

On the other hand, the fault radius given by BRUNE (1970) shows the relation of

$$a=2.34\beta/2\pi f_c\,. \tag{5.5}$$

Then the fault radius determined from Brune's formula is about 1.8 times greater than that determined from Madariaga's formula. Considering the number of earthquakes and the total swarm area estimated earlier, the fault radius by formula (5.5) seems to be too large. We shall use hereafter Madariaga's formula for the estimation of fault radius. The source radii for 19 earthquake families lie between about 120 and 200 meters (see Table 1 in TSUJIURA, 1979a).

For the circular crack, ESHELBY (1957) and KEILIS-BOROK (1959) also give the relation between the seismic moment (M_0) and stress drop ($\Delta\sigma$)

$$\Delta\sigma=\frac{7}{16}\frac{M_0}{a^3}\,. \tag{5.6}$$

The stress drop obtained using Madariaga's fault radius shows the values of 2.6 bars for $M=1.5$ and 80 bars for $M=3$ earthquakes, respectively.

Using the moment and source radius obtained above, the value of slip length (dislocation) is determined by Brune's formula

$$\Delta U=\left(\frac{2\pi}{3}\mu a^2\right)^{-1}M_0 \tag{5.7}$$

where ΔU is the slip length and μ is the rigidity. The values of slip for 266 events including a specially large earthquake of $M=5.4$ were estimated assuming $\mu=3\times10^{11}$ dyne/cm^2 (TSUJIURA, 1979a). There is some correlation between the source size and the slip length. For a given source size, the slip length cannot exceed a limited value. Our estimation of the maximum slip is 3.5 cm for 120 meters and 50 cm for 1 kilometer source radius, respectively.

5.4b. Earthquake swarm in northern Tokyo Bay in 1979

An earthquake swarm occurred in northern Tokyo Bay during the period from July 11 to August 3, 1979. The seismograms throughout the swarm sequence showed similar waveforms belonging to one earthquake family (Fig. 4.5). Sixteen earthquakes with moderate-size amplitudes on filtered-seismograms at two stations were studied on the basis of the spectral analysis. The magnitudes of these events lie between 1.8 and 3.0.

The source spectra obtained from S waves at TSK and OYM assuming the values adopted by TSUJIURA (1980) are shown in Fig. 5.6. The approximate corner frequencies are indicated by arrows. These corner frequencies show the same value, independent of the absolute values of amplitudes, though there are minor differences in the shape of high frequency components. Using this corner frequency, the source radius (a) which was determined from formula (5.4) shows a value of about 120 meters. From flat levels at low frequencies, the estimated seismic moment (M_0) are, on the average, 2×10^{19} dyne cm for $M=1.8$

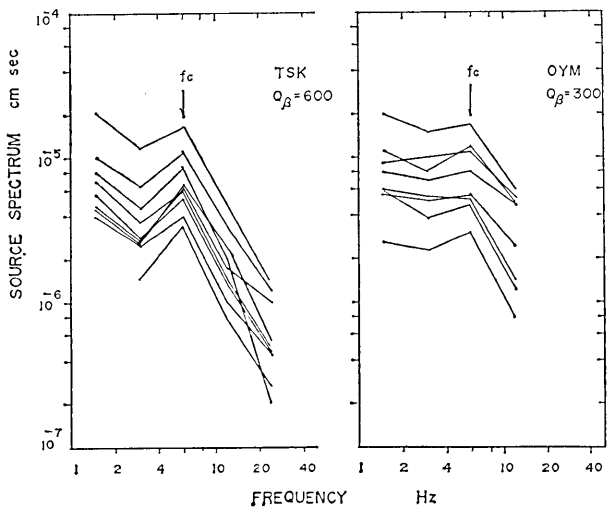

Fig. 5.6. Source spectra obtained from S waves at TSK and OYM for the earthquake swarm in northern Tokyo Bay.

and 3×10^{20} dyne cm for $M=3$ earthquakes, respectively. From the values of M_0 and a obtained above, the estimated stress drops show values of 5 bars for $M1.8$ and 80 bars for $M3.0$ earthquakes, respectively. It is noted that the stress drop is roughly proportional to the seismic moment within a limited magnitude range.

As shown in Chapter 4.4, the epicenters of these earthquakes are distributed within a spatial dimension of about 400 meters migrating systematically with time. Considering the source size of each event and the epicentral area, it is expected that these earthquakes occurred on the same fault plane as repeated slipping, because it is rather difficult to imagine that many earthquakes with a source radius of 120 meters occur independently on different faults within an area of 400 meters.

5.4c. Earthquake swarm off the east coast of the Izu Peninsula in 1980

As mentioned in Chapter 4.3c, this earthquake swarm contained many bursts of activity, each of which consisted of earthquakes with several families. The spectral analysis of earthquakes belonging to 12 families was made by the same procedure described in the previous sections.

Figure 5.7 shows the filtered-seismograms obtained at DDR for the events belonging to one earthquake family. According to RAUTIAN

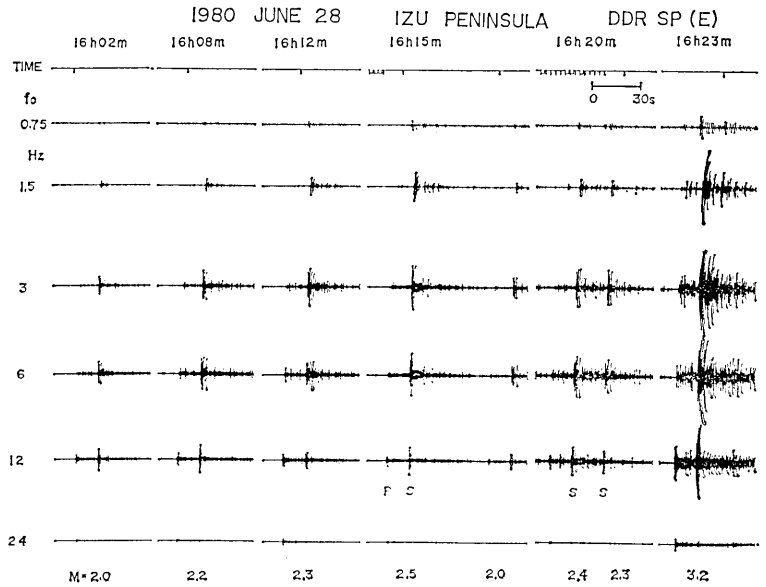

Fig. 5.7. Examples of the filtered-seismograms for the events belonging to one earthquake family. f_0; center frequency of each band-pass filter with one octave bandwidth. Tick marks at the top are minute marks.

and KHALUTRIN (1976) and AKI (1980a) with regard to the relation between Fourier spectrum and band-pass filter spectrum, Aki and Chouet's method (AKI and CHOUET, 1975) may not be applied in the case of non-impulsive waveform. In our seismograms presented in Fig. 5.7, S waves for two channels centered at 3 and 6 Hz show non-impulsive waveforms consisting of a few cycles of oscillation with comparable amplitudes. The $|F(\omega)|$ of these channels estimated by the fore-mentioned method therefore will give an underestimation by a factor roughly equal to the square root of the number of cycles in the wave train (AKI, 1980a).

Despite these uncertain seismograms, some differences in the spectra between different families can be found. Figure 5.8 shows the filtered-seismograms belonging to another family. The amplitude ratio for 6 and 3 Hz bands of these earthquakes is at least double that shown in Fig. 5.7.

Using these seismograms, the source spectra corrected for the attenuation and the site factor are obtained. The source spectra of earthquakes belonging to two families are shown in Fig. 5.9. The corner frequencies of events in each family show similar values, independent of the absolute values of amplitudes. As discussed earlier, however, the amplitudes in low-frequency bands give an underestima-

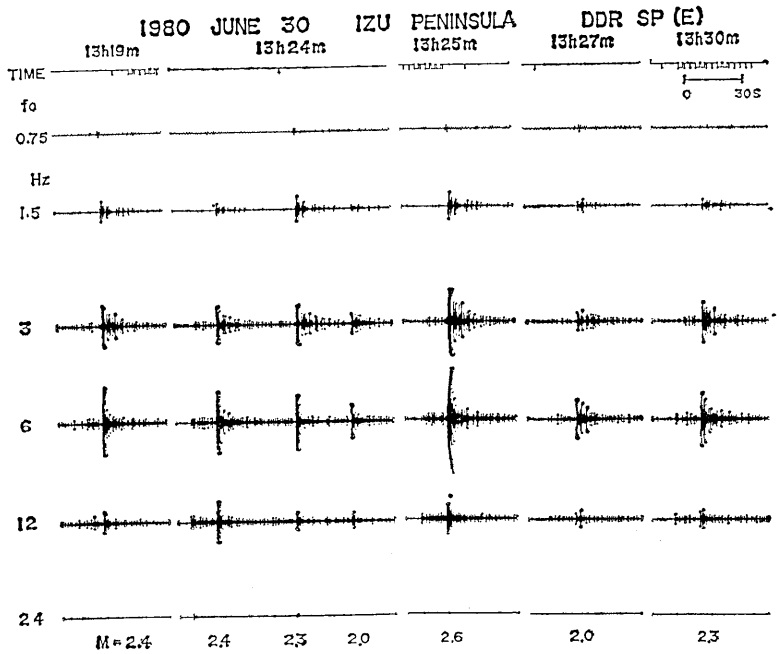

Fig. 5.8. Examples of the filtered-seismograms for the events belonging to one earthquake family. The amplitude ratio of 6 Hz/3 Hz is double that shown in Fig. 5.7.

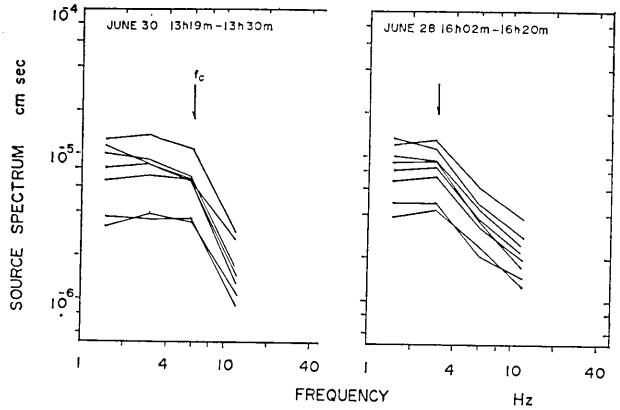

Fig. 5.9. Comparison of the source spectra of two earthquake families. The corner frequencies are different by a factor of two between the families.

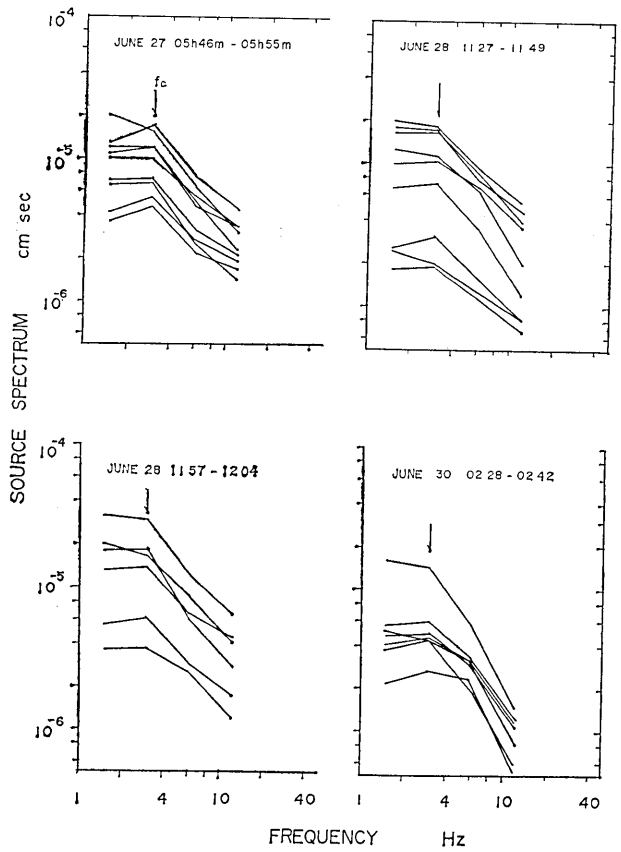

Fig. 5.10. Source spectra of small earthquakes preceding a large earthquake with $M \geqq 4.5$.

tion. Considering the uncertainty of the seismograms shown in Fig. 5.7, the long-period level gives an underestimation of roughly a factor of 0.5. The corner frequency therefore may be overestimated. Even if this uncertainty is not taken into account, there exists a clear difference in the source spectra between the family which can be attributed to the difference of corner frequency. The corner frequency obtained here lies between 3 and 6 Hz.

Fig. 5.10 shows the source spectra of other groups of families. Each family consists of events preceding a large earthquake with $M \geqq 4.5$. The corner frequencies of these groups are low, about 3 Hz, without exception.

Table 5 shows the distribution of the corner frequencies of events with $M \cong 2.5$ for 12 families. The magnitude of the largest earthquake included in each family is also shown for comparison. It is interesting to note that there is some correlation between the corner frequency and the size of the largest event. The family with a low corner frequency, on the average, contains a larger event than a family with a high corner frequency. Further discussion of this problem will be given in a later section.

As mentioned in Chapter 4.3c, the earthquakes in a family are distributed over a magnitude range from 2.0 to 4.9. In order to know the spectral feature of the whole family, seismograms of the medium-period seismograph (MP) recorded on magnetic tapes are used for a large event ($M > 3.2$), because our short-period seismograph has a limited dynamic range. The spectral analysis using the band-pass

Table 5. Distribution of the corner frequency (f_c) of earthquakes with $M \cong 2.5$ for 12 earthquake families. M_{max}; magnitude of the largest earthquake in each family. The time indicated in brackets shows the occurrence time of the largest earthquake.

Date	Time		f_c	M_{max}	(Time)	
	h m	h m	Hz		h	m
June 25	21 50	— 22 40	5	2.9	22	00
June 27	05 43	— 06 14	3	4.9	06	06
June 28	02 33	— 03 00	4.5	3.5	03	00
June 28	11 47	— 12 20	3	4.9	12	05
June 28	16 02	— 16 47	3	3.8	16	47
June 29	01 18	— 01 27	3	3.7	01	22
June 29	12 08	— 12 31	6	3.1	12	24
June 30	13 13	— 13 30	6	2.9	13	20
June 30	18 15	— 18 36	6	3.2	18	36
July 2	18 48	— 20 30	6	3.0	19	53
July 5	07 58	— 08 55	6	3.3	08	25
July 6	14 07	— 14 35	3	4.1	14	19

filters with 1/3 octave bandwidths is made for large events included within the family.

Figure 5.11 shows the source spectra obtained from S waves of large events comparing with the source spectra of small events obtained earlier (dashed lines). The seismograms after S waves of three events are also shown for comparison. From the combined data of small and large events, we constructed the scaling law of the source spectra for whole earthquake family. The corner frequencies are nearly constant within a range of 2.6 and 3 Hz over the magnitude range from 2.0 to 4.6, though the high frequency asymptote has a steeper slope for a M4.6 than for a M3.2 event.

As pointed out earlier, however, our interpretation of the S-wave

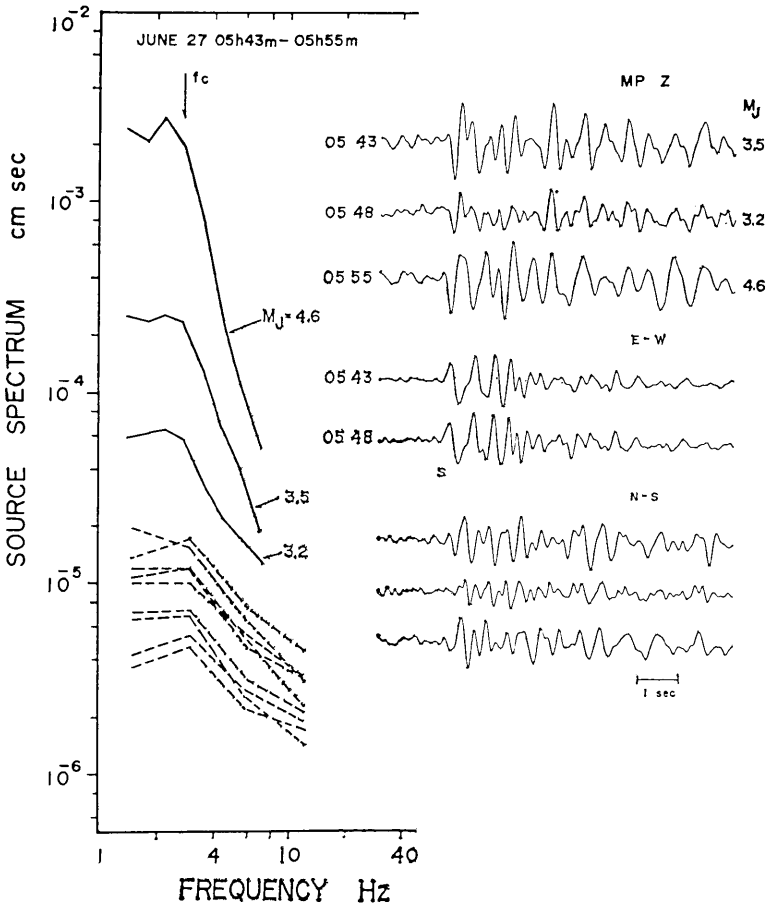

Fig. 5.11. Source spectra of events belonging to one earthquake family and the seismograms of three events with $M \geqq 3.2$. Magnitudes of these events lie between 1.8 and 4.6. The corner frequencies (f_c) are nearly constant within a range of 2.6 and 3 Hz, though the steepness of high frequencies increases with magnitude.

spectra has some uncertainty when they have non-impulsive waveforms. In order to examine the effect described above, the Fourier analysis is made for corresponding waves using the Analyzer (model 3112) of Kanomax Co. LTD. Figure 5.12 shows the Fourier amplitude spectra obtained from *S* waves with time interval of 5 sec for the same events shown in Fig. 5.11. The spectrum of microtremor including the instrumental noise of the recording system is also shown for comparison. It is confirmed that the frequency of the spectral peak is the same with a value of 2.5 Hz for events with magnitudes 3.5 and 4.6, and the high frequency amplitudes ($f > 3$ Hz) for a M3.5 event are larger than those for a M4.6 event. Similar spectral shapes were found from the Fourier analysis of the near-field acceleration seismograms with comparable magnitudes (TANAKA *et al.*, 1980). Thus, it may be concluded that the corner frequency of the events in a family is nearly the same within a limited magnitude range. Such spectral features are quite different from those expected from the ordinary scaling law of seismic source spectra (AKI, 1967, 1972), the dependence of spectra on magnitude (TSUJIURA, 1973b) and the relation between the period of initial motion and earthquake magnitude (TERASHIMA, 1968). This disagreement may be mostly due to the difference in the source process. Familiar earthquakes occur over the same fault plane bounded by barriers, and the

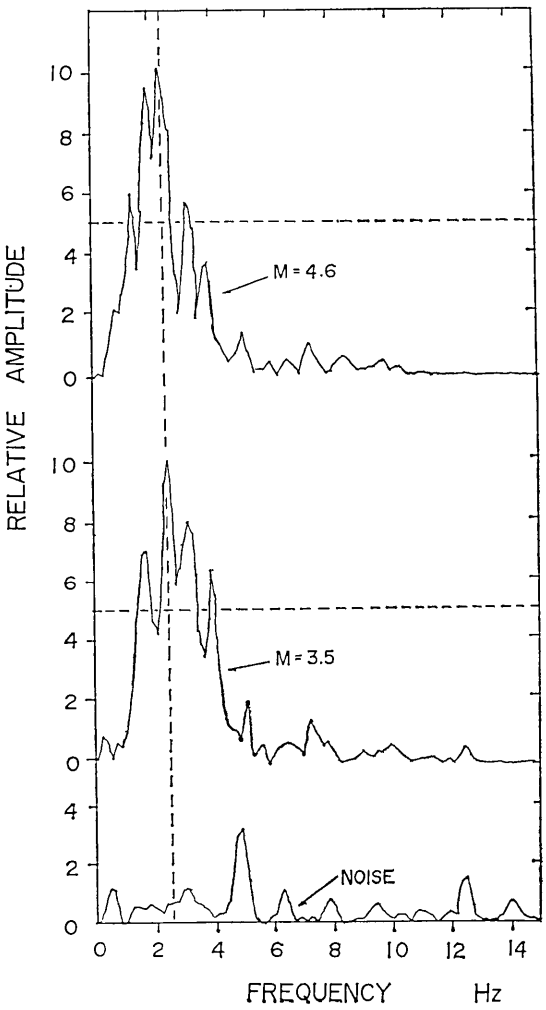

Fig. 5.12. Fourier amplitude spectra of the same events shown in Fig. 5.11. Spectrum of microtremor including the instrumental noise is also shown for comparison.

difference of earthquake size may be caused by the difference of the average slip length over the fault plane.

The path of constant corner frequencies and the difference of the steepness of spectral curves at high frequencies can be explained also by the model of rupture propagation in a heterogeneous medium proposed by DAS (1976). The crack tip propagates smoothly over the fault plane and stops because of high strength barrier. This mechanism corresponds to the $M4.6$ earthquake. Consider now the case where there are obstacles along the fault, the rupture front can pass through these obstacles without breaking them. In such a case, the fault slip is small, but the corner frequency is the same as in the case of smooth propagation. This mechanism corresponds to the $M3.2$ earthquake. According to DAS (1976), the high-frequency versus low-frequency content of the spectrum is also large for ruptures with barriers than for smooth ruptures.

Using the circular crack model of MADARIAGA (1976), the source radius (a) for the events shown in Fig. 5.11 was determined and a value of about 250 meters is obtained. From flat low-frequency level (Ω_0), the corresponding seismic moment (M_0) was determined by using formula (5.3), assuming the values adopted by TSUJIURA (1979a). The result shows an average seismic moment of 1×10^{20} dyne cm for $M=2.0$ and 5×10^{22} dyne cm for $M=4.6$ earthquakes, respectively. From the M_0 and a obtained above, the value of stress drop was estimated by using formula (5.6). Their results show values of 3.5 bars for $M2.0$ and 650 bars for $M4.6$ earthquakes, respectively. The stress drop obtained using a radius of Madariaga's formula is about six times greater than that using Brune's formula. Even considering the difference of our estimation, the stress drop of the $M4.6$ earthquake shows a greater value than those estimated earlier by the use of crack models (THATCHER and HANKS, 1973; ISHIDA, 1974; JOHNSON and MCEVILLY, 1974; TSUJIURA, 1978b). Thus, we may conclude that an earthquake of $M4.6$ occurred as the maximum stress drop earthquake in a given fault. Because of this large stress drop, all the available stress may be released and no more aftershocks follow (see Figs. 10 and 11 in TSUJIURA, 1981).

Through the swarm sequence, eight events with magnitudes around 4.6 were observed, but no earthquakes were found above $M5.0$, except for the $M6.7$ sequence which shows a different activity mode (TSUJIURA, 1981). The reason for the absence of an extremely large earthquake may partly be due to the limited available stress drop. As shown earlier, the corner frequencies for events in one earthquake family are nearly constant within a range from 2.6 and 3 Hz for magnitudes between 2.0 and 4.6. This evidence suggests that the stress drops of

events belonging to one family are proportional to the earthquake size (seismic moment). Our estimation of the maximum stress drop showed a value of about 650 bars for a $M4.6$ earthquake. If there occurs an event with $M5$, the stress drop may exceed 1 kbar. Such a value would be too large for the stress drop of a crustal earthquake. In other words, the fault area of this earthquake family is too small for a $M5$ earthquake. In fact, we found several earthquake swarms supporting the above conclusion.

5.5. Prediction of the largest earthquake

Through the spectral studies of three earthquake swarms we found that the corner frequencies in a given earthquake family are nearly constant and their values are defined by the size of the largest event included within the family. In order to confirm the above conclusion, further studies will be made for other swarm sequences. In this study, however, a comparison of earthquake swarms which occurred in the same area is more appropriate because the effect of attenuation along the propagation path is common. We selected, for this purpose, the earthquake swarms in following three areas, northern Izu Peninsula (Nos. 9, 14 in Table 1), off Ibaraki Prefecture (Nos. 8,

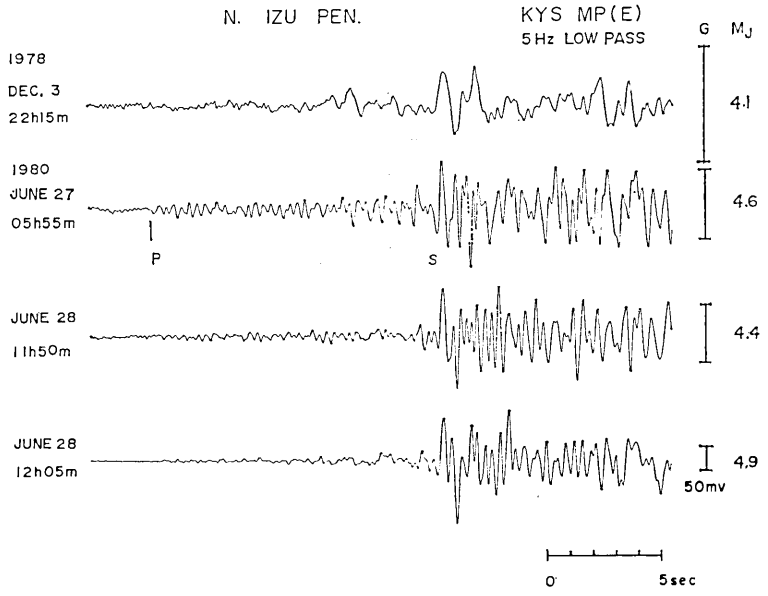

Fig. 5.13. Comparison of the seismograms obtained by the medium-period seismograph (MP) at KYS for the two swarm sequences in the northern Izu Peninsula. The 1980 sequence is the largest event in each family and the 1978 sequence is the event preceding the main shock with M=5.4. Low frequency waves in the 1978 seismogram are more predominant than those in the 1980 seismograms. G; relative difference of the gain of play-back amplifier from magnetic tape.

13) and east off Chiba Prefecture (Nos. 5, 7).

Figure 5.13 shows a comparison of seismograms for two swarm sequences obtained by the medium-period seismograph (MP) at Kiyosumi station (KYS). The lower three seismograms show the largest event in each family taken from the 1980 earthquake swarm in the Izu Peninsula and the other shows the event belonging to the family with the largest event of $M=5.4$ which occurred during the 1978 swarm sequence in the same area. The seismogram of the 1978 swarm shows remarkably low-frequency waves in spite of its smaller magnitude.

Figure 5.14 shows the source spectra of these events obtained from S waves at KYS, assuming the values of $Q_\beta=300$ and $V=4.2$ km/sec. The corner frequency between two sequences differs at least by a factor of three and its value depends on the size of the largest event included within the family. The choice of Q_β, however, may affect the estimation of the corner frequency. Focal coordinates for these events by JMA are given in Table 6. Their epicenters cluster within an area of about 10 km and are located at the same distance, about 100 km, from KYS. Considering the epicentral distance, the dimension of the epicentral area and the frequency range concerned,

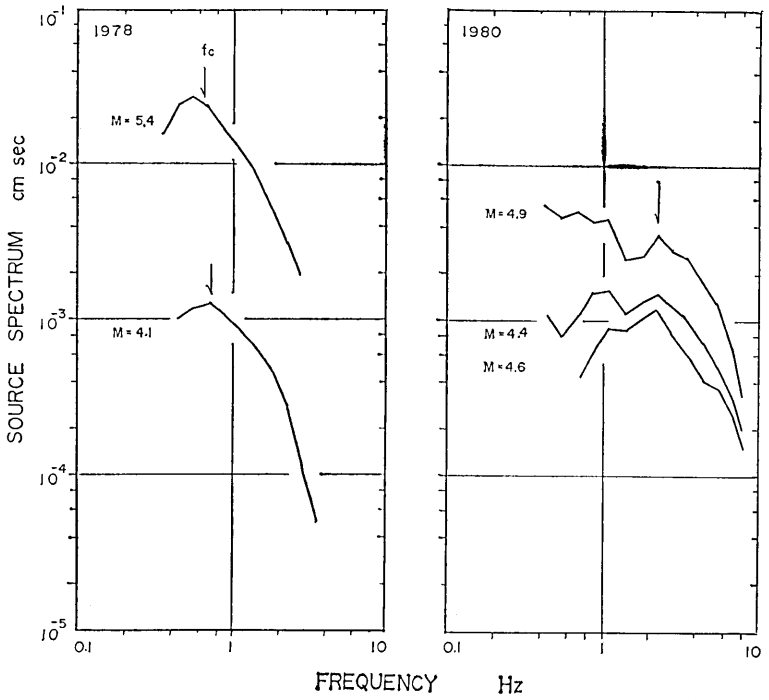

Fig. 5.14. Comparison of source spectra for two swarm sequences shown in Fig. 5.13. Note that the corner frequency depends on the size of the largest event within the family.

Table 6. List of focal coordinates. h; source depth, M; magnitude.

Date	Time			Long., E			Lat., N			h	M
	h	m	s	D	M	M	D	M	M	km	
1978 Dec. 3	22	15	00.3	139	08	00	34	53	00	00	4.1
1980 June 27	05	55	06.5	139	13	01	34	56	01	00	4.6
1980 June 28	11	50	42.5	139	12	00	34	57	00	00	4.4
1980 June 28	12	05	02.0	139	12	01	34	56	01	00	4.9

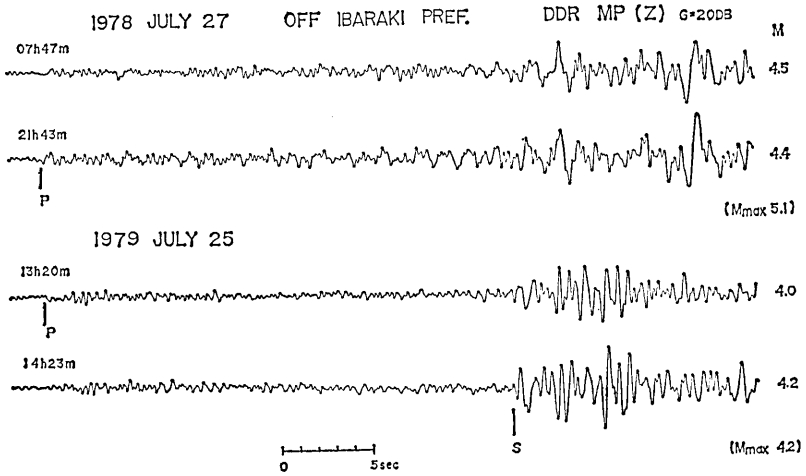

Fig. 5.15. Comparison of the seismograms with similar magnitudes obtained by the MP seismograph at DDR for the two swarm sequences off Ibaraki Prefecture. Low-frequency waves in the 1978 seismograms are more predominant than those in the 1979 seismograms. M_{max}; magnitude of the largest event in each swarm sequence.

the difference of corner frequencies may reflect the inherent nature of the source spectra rather than the local variation of Q_β.

Figure 5.15 shows a similar comparison of seismograms obtained by the MP seismograph at DDR for two earthquake swarms off Ibaraki Prefecture. The upper two seismograms are the events belonging to the family with the largest event of $M=5.1$ and the lower two seismograms are that of $M=4.2$. In spite of the small difference in magnitude ($\Delta M=0.2$), clear differences of the spectral contents are apparent between the upper and lower two seismograms. For example, the seismograms belonging to the family of $M5.1$ are apparently more abundant in low-frequency waves than those of $M4.2$.

Figure 5.16 shows the source spectra of two families, assuming the values of $Q_\beta=400$ and $V=4.5$ km/sec. It is also evident that the corner frequency depends on the largest event the same as that obtained for the earthquakes on Izu Peninsula. The epicenters of these events are located in almost the same direction from DDR with distances of about 235 and 260 km (Fig. 4.2). The events at a further

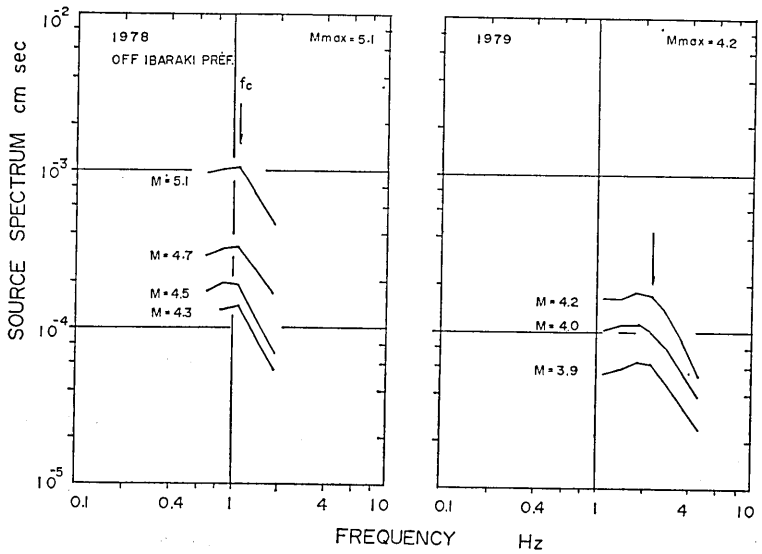

Fig. 5.16. Comparison of source spectra for the two swarm sequences off Ibaraki Prefecture. M_{max}; magnitude of the largest event through the swarm sequence. Note that the corner frequencies (f_c) of two sequences are different by a factor of about two and their values depend on the size of the largest earthquake within the sequence.

distance correspond to the high-frequency events. The difference of the corner frequency therefore is the result from the difference of the source spectra rather than the difference of Q_β between the two epicentral areas.

Similar behavior of waveforms can be seen for the earthquake swarms east off Chiba Prefecture. Figure 5.17 shows a comparison of seismograms with similar magnitudes ($\Delta M = 0.2$) for two swarm sequences. The magnitude of the largest earthquake in the group of the upper two seismograms is 5.2 while that of the lower two seismograms is 6.1. Although no clear S waves are observed for both sequences, the spectral contents of S waves in the lower seismograms are apparently more abundant in low-frequency components than in the upper two seismograms.

Figure 5.18 shows the source spectra obtained from S waves, assuming $Q_\beta = 300$ and $V = 4.5$ km/sec. The corner frequency in a given family (swarm) again shows a nearly constant value, and its value depends on the size of the largest event included within the family.

The loci of corner frequencies for the families are summarized in Fig. 5.19. Numerals attached to the solid lines refer to the swarm numbers listed in Table 1. Through the analysis of the spectra of earthquake swarms in different areas, it is confirmed that the corner frequencies in a given family are nearly constant within a limited

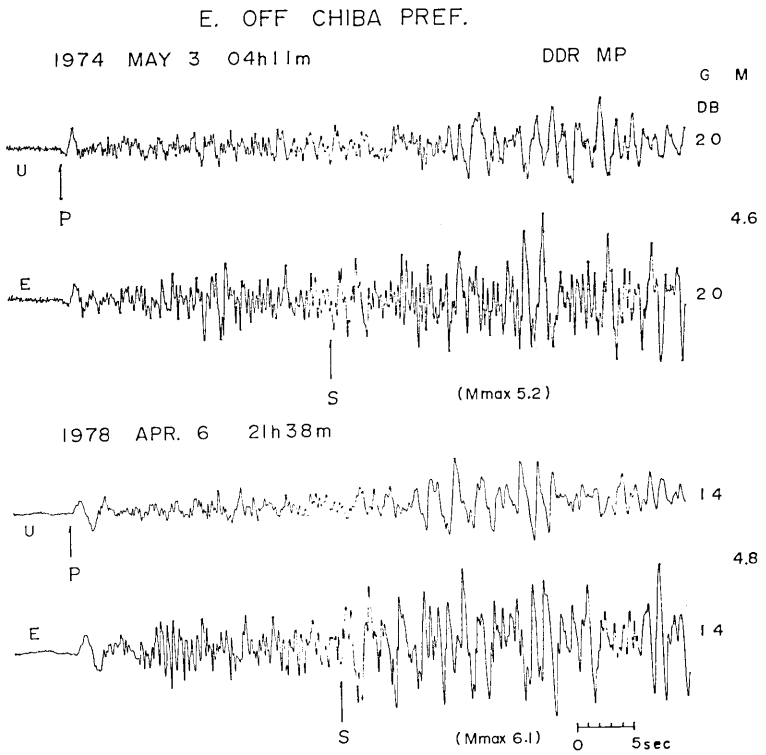

Fig. 5.17. Comparison of the seismograms with similar magnitudes obtained by the MP seismograph at DDR for the two swarm sequences east off Chiba Prefecture. Low-frequency waves in the 1978 seismograms are more predominant than those in the 1974 seismograms. M_{max}; magnitude of the largest event in each sequence.

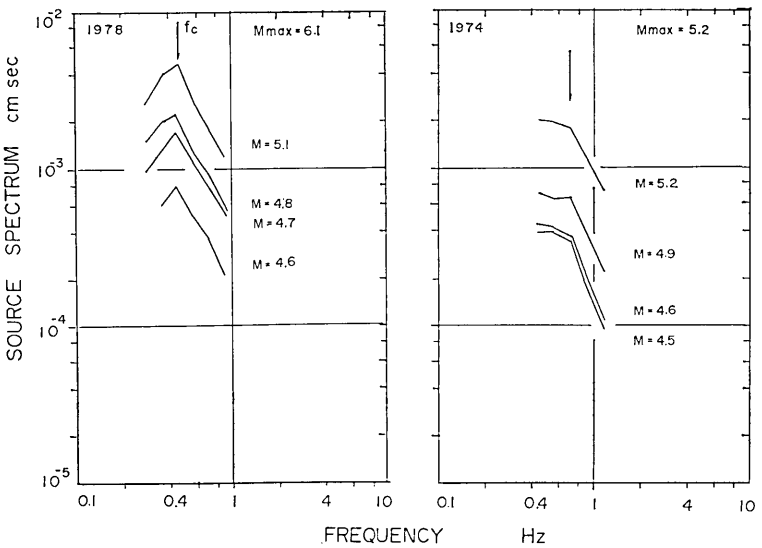

Fig. 5.18. Comparison of source spectra for the two swarm sequences east off Chiba Prefecture. M_{max}; magnitude of the largest event in each swarm sequence. Note that the difference of corner frequencies between two sequences.

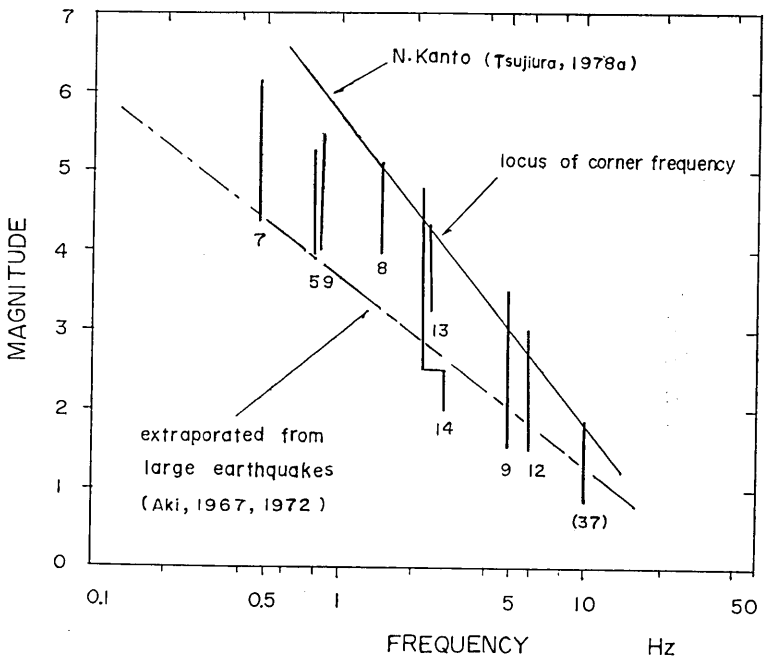

Fig. 5.19. The loci of corner frequencies as a function of magnitude for the earthquake families. Numerals attached to lines refer to the swarm number listed in Table 1. The path of corner frequencies of each sequence shows a straight line with a constant corner frequency, and its value depends on the size of the largest earthquake in each swarm. The loci of corner frequencies extrapolated from Aki's model and the data in northern Kanto area are also indicated. The corner frequency of No. 37 is taken from the earthquake family in the ordinary seismic activity (see section 6.5).

magnitude range and their values depend on the size of the largest events within the family.

The extrapolation of the loci of corner frequencies from large earthquakes by AKI (1967, 1972) and the locus of corner frequencies derived from the scaling law of earthquakes in northern Kanto area (TSUJIURA, 1978a) are also shown for comparison in Fig. 5.19. As shown in this figure, there is a marked difference in the scaling law between Aki's model and the present study. In Aki's model the corner frequency is inversely proportional to the fault length, and the seismic moment is proportional to the cube of the fault length. Thus, the locus of corner frequencies lies on a straight line with a slope of -3.

In the present study, the locus of corner frequencies in the family shows a straight line with a constant corner frequency. This line implies a constant source dimension independent of the earthquake size. The stress drop therefore increases with magnitude along this line. However, as seen in this figure, there is some limitation of the

earthquake size in a given family. For example, the upper limit of earthquake with 6 Hz corner frequency is about $M=3$ and that of 0.5 Hz is about $M=6$. Such behavior is understandable if we assume that there is a unique length characterizing the heterogeneity of the earth's crust and the corner frequency is defined by the length of the heterogeneity in that area. The line of constant corner frequency, however, cannot be kept indefinitely with increasing magnitude because the stress drop cannot increase indefinitely. Our estimation of maximum stress drop lies about 80 bars for $M=3$ and about 650 bars for $M=4.6$ earthquakes, respectively. In other words, for a given characteristic size of heterogeneity, an earthquake beyond a certain size cannot be produced.

As mentioned in Chapter 4, the largest earthquake in a given family usually occurs in the later stage of its sequence. Considering the mechanism of the earthquake occurrence described above, continuous monitoring of the spectrum and the waveform suggests the possibility of predicting the largest earthquake in a given swarm sequence.

The locus of corner frequencies obtained from the top earthquakes in each line shows a slow rate of decrease in corner frequency with an increase in magnitude from 10 Hz for $M=2$ down to about 0.5 Hz at $M=6$. The apparent good fit of the locus of corner frequencies follows a straight line with steeper slope of -5 indicating a very slow rate of increase in the source dimension. This is nearly the same for the scaling law obtained from the mantle earthquakes (40–70 km) in the northern Kanto area where high stress drop earthquakes were observed (TSUJIURA, 1978a).

5.6. Conclusion

Through the spectral analysis of earthquake swarms, salient features of the source spectrum which differ from other activities were found. The main results are as follow:

(1) The source spectra of earthquakes in a given family show similar waveforms maintaining a constant corner frequency.

(2) The corner frequency of the earthquake in a certain size depends on the size of the largest earthquake included within the family.

(3) The size of the largest earthquake in a given family is controlled by the stress drop. The maximum stress drop obtained here is about 80 bars for $M=3$ and about 650 bars for $M=4.6$ earthquakes, respectively.

Considering the activity mode of earthquake swarms mentioned in the previous chapter, continuous monitoring of waveform and spectrum provides some useful information for the identification of earthquake

swarm and for the prediction of the size of largest earthquake in a given swarm sequence.

CHAPTER 6

Differences in the Activity Mode between the Earthquake Swarm and Other Seismic Activities

6.1. Introduction

In the previous chapters, the waveform and spectral features of earthquake swarms were clarified. If such features are different from those of other activities, such as the foreshock activity preceding a large earthquake and an ordinary (background) seismicity, present results may be useful for distinguishing those activities. Some differences in the similarity of waveforms and in the spectral characters between foreshocks and earthquake swarms or the ordinary seismicity have been made in previous studies of this series (TSUJIURA, 1977, 1979b). Including some new data, we shall again discuss this subject by studying the waveform and spectrum of foreshocks on the basis of their spatial distributions.

Although there is no established definition of foreshock, foreshocks used here refer to an activity preceding the main shock by hours or days. Since the establishment of our seismic network, several series of foreshock activities have been observed for moderate earthquakes ($M \geqq 5.4$) in the Kanto district (TSUJIURA, 1977; TSUMURA *et al.*, 1978). Among them, the foreshock activity of the 1978 Izu-Oshima-kinkai earthquake ($M=7.0$) was very active. The foreshock activities of other sequences, however, were relatively weak, and no examination of waveform was made except for the spectral study of small events (TSUJIURA, 1977). We shall deal here mainly with the foreshocks of the 1978 Izu-Oshima-kinkai earthquake.

6.2. Waveform feature of foreshocks

Figure 6.1 shows the seismograms of foreshocks with $M \geqq 3.4$ and the main shock for the 1978 Izu-Oshima-kinkai earthquake obtained by the medium-period (MP), wide-band (WB), long-period (LP) and ultra long-period (ULP) seismographs at DDR. Eleven foreshocks were observed during about 16 hour period prior to the main shock. Among these, seven events with similar magnitudes ($M=3.4$-4.1) were selected in order to examine the similarity of waveform.

Figure 6.2 shows the MP seismograms of these events reproduced at a paper speed of 10 mm/sec from magnetic tapes. The amplitude of each event is almost normalized by changing the gain of play-back

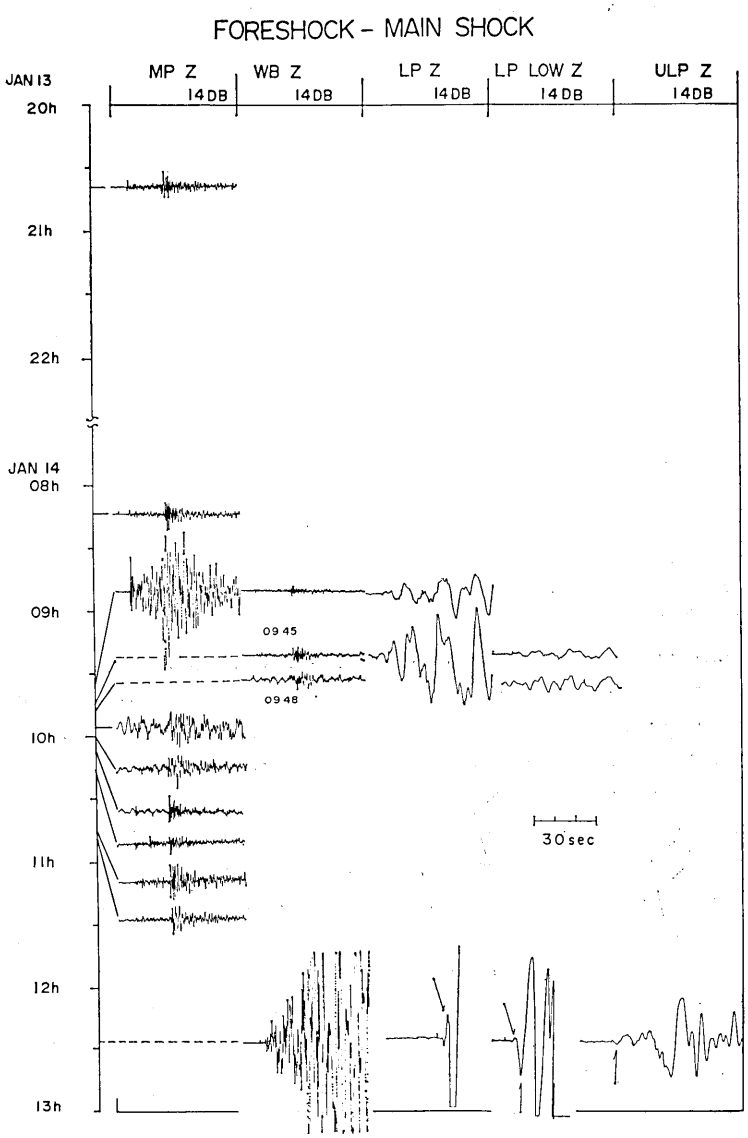

Fig. 6.1. Seismograms in the foreshock sequence with $M \geqq 3.4$ and the main shock recorded on the vertical component (Z) of four kinds of seismographs at DDR. MP: medium-period, WB: wide-band, LP: long-period (LP-Low means low magnification LP, by a factor of 1/10 for LP), ULP: ultra long-period seismographs.

amplifier (G). It is clearly seen that the waveforms are different from one event to another, and the group with similar waveforms as shown in earthquake swarms cannot be recognized. The S-P times of these events also vary in the range of 1.5 sec. The diversity of waveforms therefore may be due to the difference of their epicentral locations. The space-time distribution of foreshocks by YAMAKAWA *et al.* (1979)

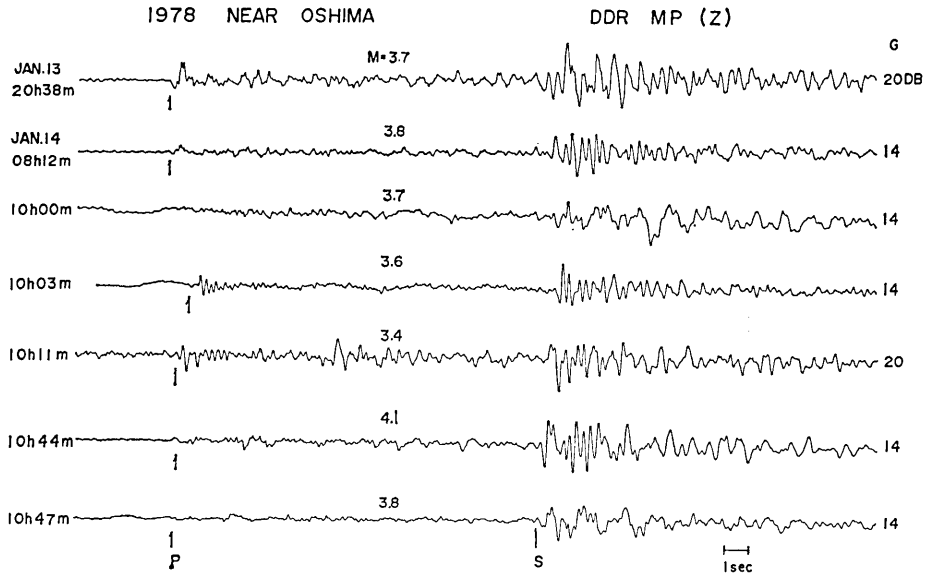

Fig. 6.2. Seismograms of foreshocks with magnitudes from 3.4 to 4.1 preceding the 1978 Izu-Oshima-kinkai earthquake.

showed that their epicenters were located within an area of about 15 km migrating systematically with time and that epicenters of immediate foreshocks tend to occur along the rupture zone of the main shock.

The area around Oshima is a place where earthquake swarms occur frequently. The two earthquake swarms which occurred near Oshima in 1972 and 1973 (Nos. 2 and 4 in Table 1) were preserved on magnetic tape at DDR. Parts of the MP seismograms of these swarms are shown in Fig. 6.3 for comparison. The striking similarity of waveforms is seen among the seismograms in contrast with the dissimilar waveforms of foreshocks in the same area.

The difference of the similarity of waveforms between the foreshock and the swarm activities can be seen more clearly when these seismograms are compared on the same figure. Figure 6.4 shows the comparison of seismograms of earthquake swarm (A) and foreshock (B) activities, each of which consists of an activity over a 50 minute period. The difference in the similarity of waveforms between the two activities is definitely recognized, though they occurred within a similar time interval. Such a difference may be partly due to the differences in the mechanism of earthquake occurrence. As mentioned in Chapter 4, the earthquake family in a swarm occurs within a very small focal area, probably on the same fault plane as repeated slipping. On the other hand, the foreshocks occur over a wide area presumably selecting weak places within the zone where the main shock will occur later. In fact, the stress drops of foreshocks show considerable

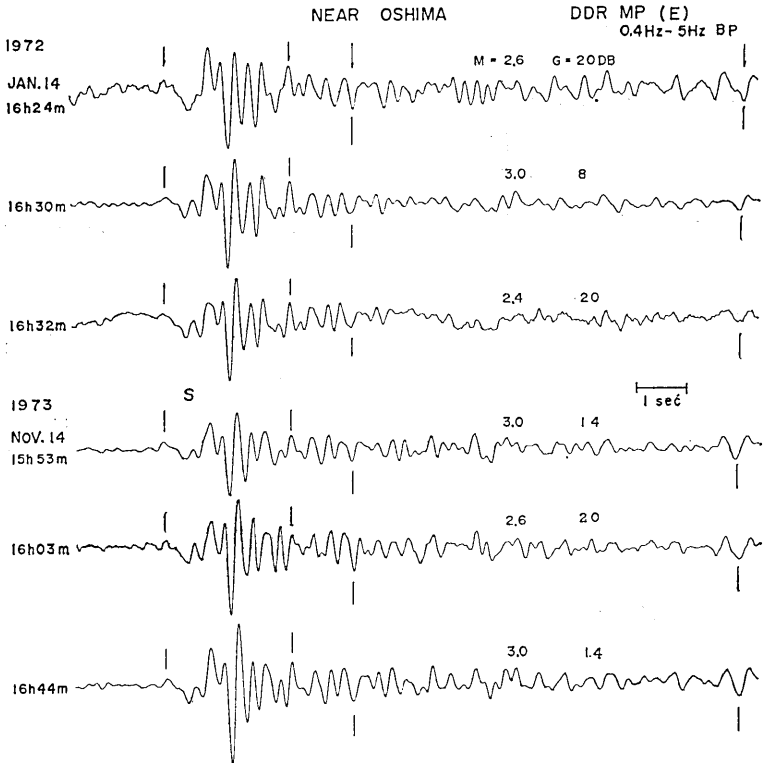

Fig. 6.3. Examples of the seismograms obtained from the earthquake swarms which occurred near Oshima.

low values as will be discussed later. The difference in waveform similarity between the two activities is also understandable if we consider the difference of the field of stress concentration. Earthquake swarms may occur in the area where the tectonic stress is concentrated locally, whereas foreshocks may occur under the stress concentration in a wide area presumably including the entire focal area of the main shock.

The diversity of waveforms can be seen also in the foreshocks preceding the earthquake off the cape of Erimo, Hokkaido on January 19, 1979 ($M=5.4$). Figure 6.5 shows the seismograms of foreshocks and aftershocks given by SUZUKI (1981). Four foreshocks with magnitudes between 2.6 and 3.8 were observed during the 17 days prior to the main shock. Of these, three events occurred during the 10 hour period immediately preceding the main shock. By comparing these seismograms it is definite that all earthquakes have an individual waveform character and no earthquake family similar to that shown in the earthquake swarms was observed. A similar feature of waveforms was seen also in the immediate foreshocks of the 1966 Parkfield,

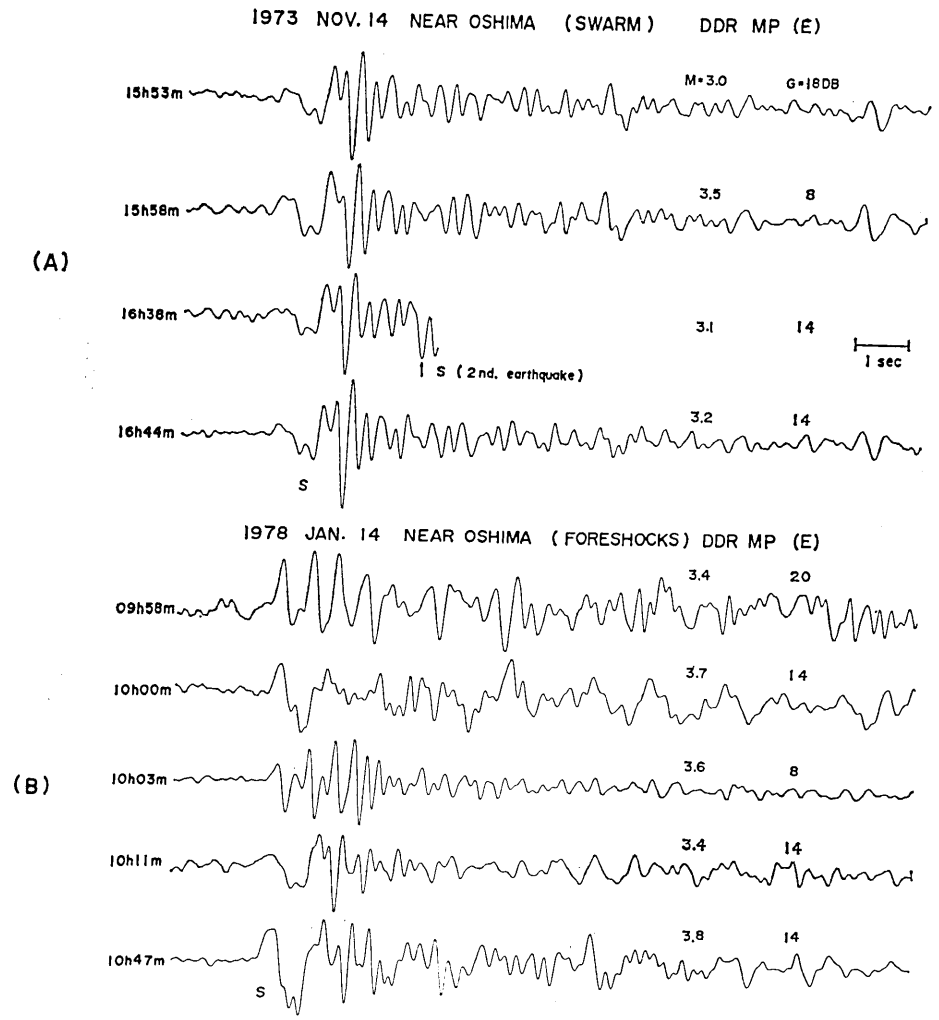

Fig. 6.4. Comparison of waveforms for the earthquake swarm (A) and the foreshocks (B) which occurred near Oshima. The difference of the similarity of waveforms between two activities is clearly recognized.

California earthquake (see Fig. 2 in BAKUN and MCEVILLY, 1979).

On the other hand, ISHIDA and KANAMORI (1978) studied the waveforms of five events which occurred during the two year period prior to the 1971 San Fernando earthquake. Considering the background seismicity, Ishida and Kanamori identified these earthquakes as foreshocks in a broad sense, and they also concluded that the waveforms of these earthquakes were remarkably similar for each event. Such behavior is inconsistent with our results. However, the pattern of the foreshock activities is clearly different between the San Fernando earthquake and the Izu-Oshima-kinkai earthquake. In the San Fernando

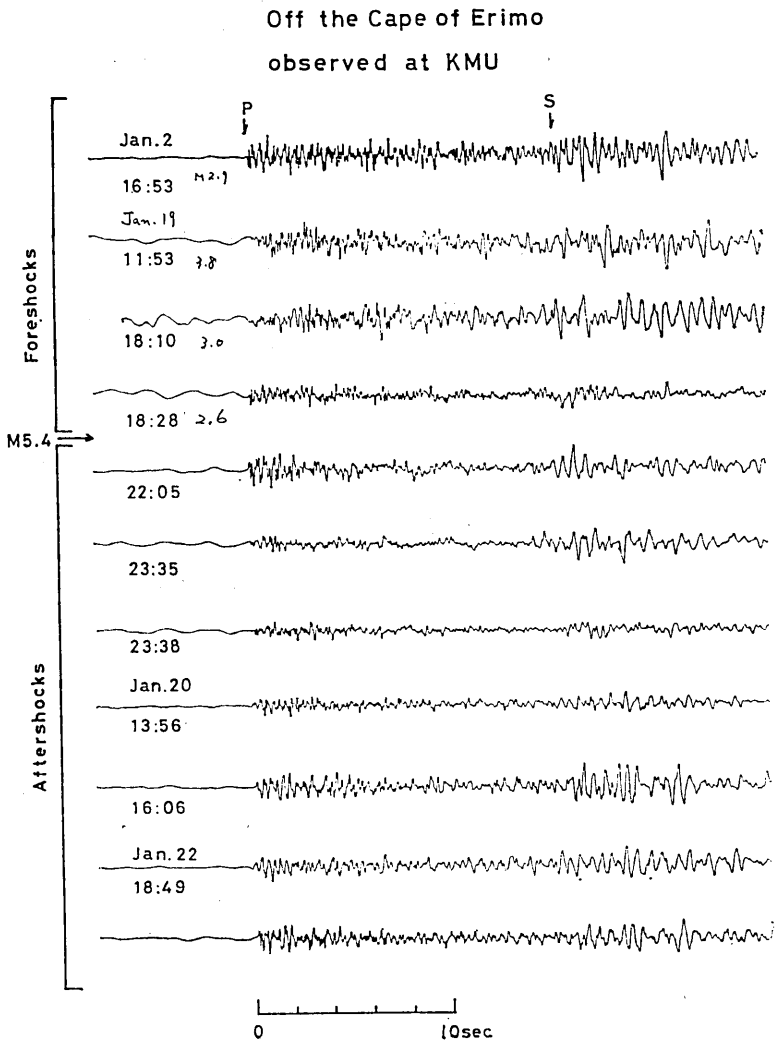

Fig. 6.5. Seismograms of the foreshocks and aftershocks of earthquake with M=5.4 off the cape of Erimo, Hokkaido.

earthquake, five events with magnitudes between 2.5 and 2.8 occurred during the two year prior to the main shock. In our case, however, pronounced foreshock activity was observed during the 10 hour period prior to the main shock. Therefore, the difference in the type of foreshock activity may be responsible for the difference of the similarity of waveforms. However, more available data will be definitely needed to evaluate the reliability of this technique.

6.3. Spectral feature of foreshocks

In order to obtain the spectral feature of foreshocks the spectral

analysis is performed for S waves by using the band-pass filters with a 1/3 octave bandwidth. We shall describe here the main results obtained from the foreshock sequence of the 1978 Izu-Oshima-kinkai earthquake.

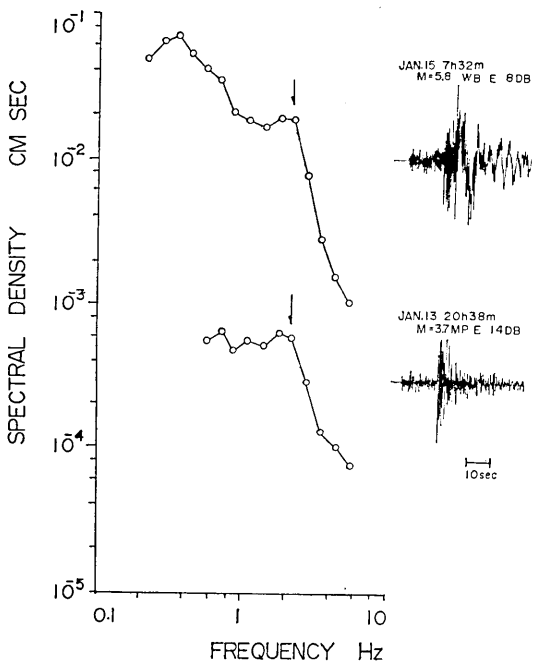

Fig. 6.6. An example of the source spectra of S waves corrected for the attenuation using the values of $Q_\beta=300$ and $V=3.5$ km/sec, and frequency-dependent site factors. Arrows show the corner frequency.

Figure 6.6 shows an example of the source spectra obtained from S waves by using the values adopted by TSUJIURA (1978b). The corner frequency of the large event ($M=5.8$) could not be determined uniquely so we assumed tentatively the corner frequency as indicated by the arrow.

From the flat low-frequency level (Ω_0) and the corner frequency (f_c) the source parameters such as seismic moment (M_0), source dimension (r) and stress drop ($\Delta\sigma$) are estimated by Brune's model, assuming the shear-wave velocity of 3.5 km/sec and the density of 2.8 g/cm^3.

Figure 6.7 shows the relation between the source dimension and the seismic moment for the foreshocks, aftershocks and ordinary seismic activity in that area (see also Table 1 in TSUJIURA, 1978b). The source dimension of foreshocks varies from one event to another even for events with similar moments, and no systematic variation in source dimension and seismic moment was obtained. ISHIDA and KANAMORI (1980) suggested that the frequency of spectral peak of foreshocks is higher than the events of ordinary background activity. However, it is concluded in the present study that the stress drop of foreshocks, on the average, takes a low value which is consistent with those of the foreshocks of the eastern Yamanashi Prefecture earthquake of 1976 and the Kawazu earthquake, Izu Peninsula of 1976 (TSUJIURA, 1977). This may be partly due to the local variation of source spectra.

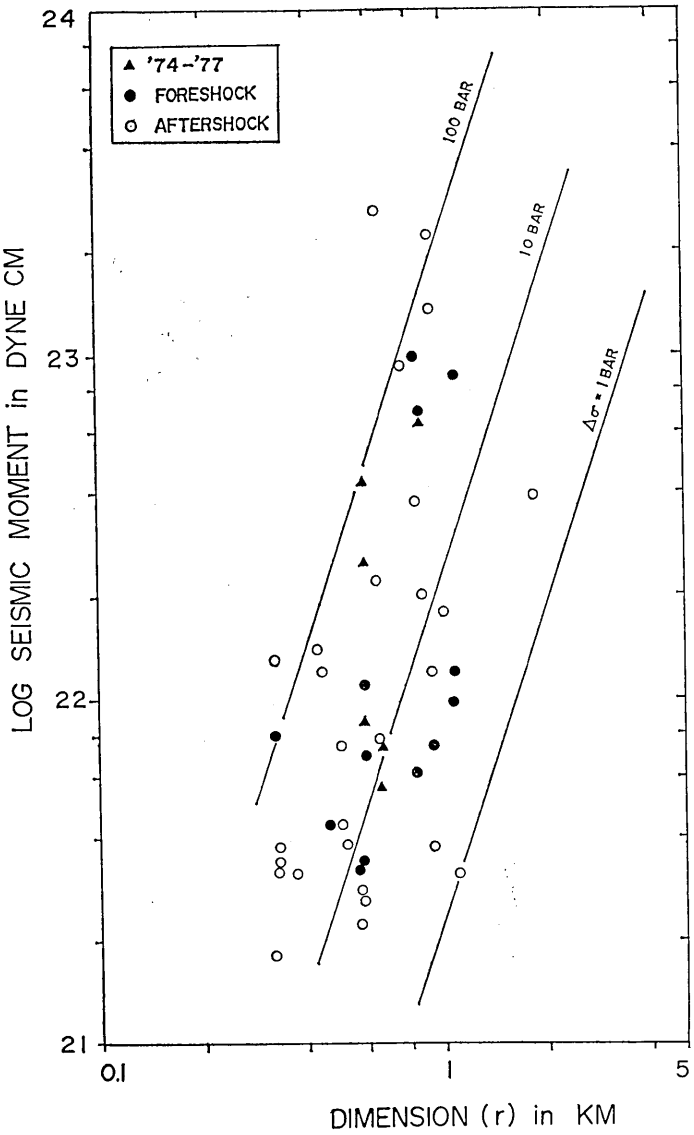

Fig. 6.7. Relation between log seismic moment and source radius derived from the corner frequency of S waves for the Izu-Oshima-kinkai earthquake sequence. Diagonal lines show constant stress drops.

6.4. Local variation of source spectra

Local or regional variations of source spectra were found in various seismic regions, and they were discussed in terms of tectonic features of the regions (WYSS and BRUNE, 1971; DOUGLAS and RYALL, 1972; THATCHER, 1972; THATCHER and HANKS, 1973; TSUJIURA, 1973b; CHOUET *et al.*, 1978). The Oshima area is located on a volcanic front where

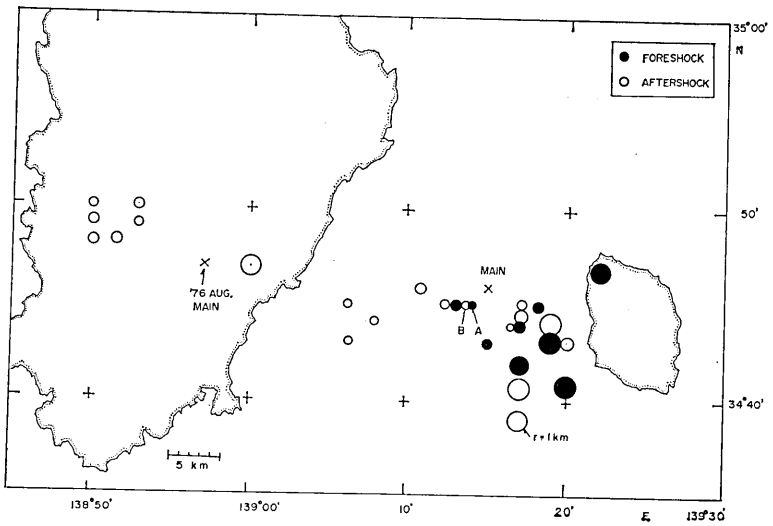

Fig. 6.8. Spatial distribution of the source size for events with M=3.5-4.1 (M_0=2×10^{21}-1×10^{22} dyne cm).

complicated media may be expected in the crust. In fact, earthquake swarms occur frequently near Oshima.

Using the epicenters given by the Japan Meteorological Agency, the source dimensions of foreshocks within a limited magnitude range (M=3.5-4.1) are shown in Fig. 6.8. We find that there is a local variation of source dimensions even within an area of about 20 km. For example, events with large source dimensions are seen near Oshima. The difference of source spectra, therefore, may be due to the difference of their locations where the static shear strength of media differs locally, and the neighboring area of Oshima may consist of the media with relatively weak shear strength. Similar local variations of source dimensions were seen also in the same areas of the Kawazu earthquake on Izu Peninsula (TSUJIURA, 1977) and the aftershock sequence of the 1978 Izu-Oshima-kinkai earthquake (TSUJIURA, 1978b).

The difference of source depth, however, may affect the source spectrum (TSUJIURA, 1969; MASUDA, 1978). The source depth of foreshocks determined by JMA lies within a range of 0 and 20 km, but there is no systematic variation of the source depth within the area concerned. The difference of source spectra obtained here therefore may reflect the inherent tectonic nature of this area rather than the local variation of source depth.

6.5. Earthquake family in ordinary seismic activity

From the analysis of waveform, it is confirmed that the earthquake swarm activity mainly consists of events with similar waveforms called an earthquake family. In order to discriminate the swarm activity

from other sequences it is important to know the nature of ordinary seismic activity in terms of similarities of waveforms.

Another important aspect of this study is to know the recurrence rate of familiar earthquakes. If familiar earthquakes occur repeatedly with a limited time interval, continuous monitoring of the waveforms and spectra makes it possible to estimate the rate of stress release or the rate of seismic slip on the corresponding fault. Recently BUFE *et al.* (1977) and SHIMAZAKI and NAKATA (1980) studied the recurrence of earthquakes in a specified area and pointed out that recurrence rates of earthquakes are roughly proportional to the amount of coseismic displacement of the preceding event.

For this purpose, we selected the seismic area in the western part of Tokyo where the activity of shallow earthquakes is relatively high (e.g., TSUMURA, 1973) and studied the waveforms in terms of similarities using the data of OYM where the seismograms are recorded at a paper speed of 25 mm/sec by a trigger mode. In this procedure, however, the reference earthquakes must be considered as the standard earthquakes. One hundred local earthquakes (S-$P \leqq 6$ sec) with different waveforms which occurred during the period from January to December, 1979, were selected as the reference earthquakes, and the existence of events with similar waveforms during a later period was examined.

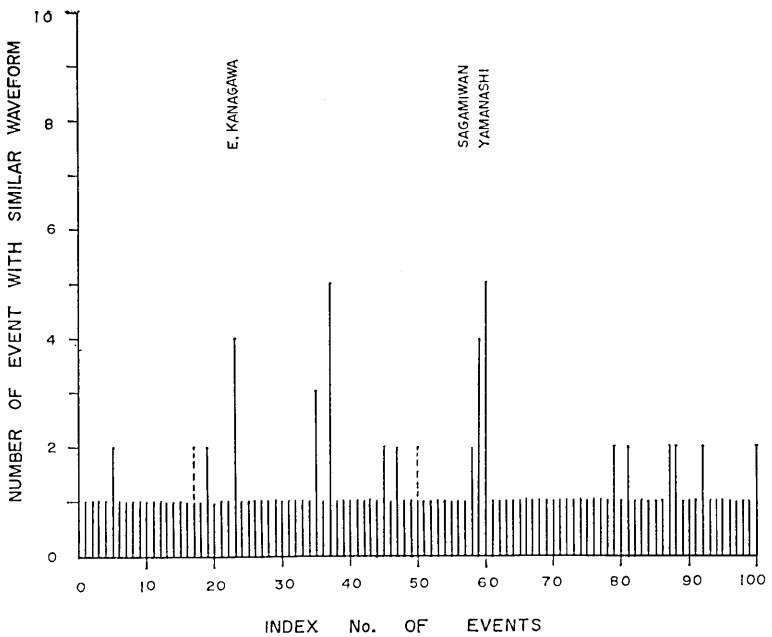

Fig. 6.9. Distribution of the earthquakes with similar waveforms in the ordinary seismic activity observed at OYM during the period from January, 1979 to June, 1981.

Magnitudes of these events lie between 0 and 3.0.

Figure 6.9 shows the distribution of earthquakes with similar waveforms for the 100 reference earthquakes selected from 450 earthquakes which occurred during the period from January, 1979 to June, 1981. It is evident that the rate of the occurrence of earthquake families is very low compared to those of earthquake swarms. Some groups with a relatively large number of similar earthquakes (Nos. 23, 59 and 60) were generated in the area where the swarm activity occurs repeatedly. Although the number of events and the observation period are insufficient, the present results show that the rate of the occurrence of an earthquake family is very low in ordinary seismic activity. Further discussion on this subject will be made following the collection of more data (in preparation).

6.6. Conclusion

Through the analyses of waveform and spectrum for the foreshock and ordinary seismic activities we found that the waveform and spectral features of these activities differ from those of the earthquake swarm. The main results are as follow:

(1) No earthquake family was observed in the immediate foreshocks preceding the main shock.

(2) The complicated pattern of the source spectra was observed for the foreshock sequence, and there is no simple linear relationship between the source dimension and the seismic moment.

(3) The rate of the occurrence of earthquakes belonging to the same family is very low in ordinary seismic activity.

Contrary to the above, as shown in the previous chapters, the earthquake swarm shows similar waveforms maintaining a constant corner frequency. Therefore, if such differences are always observed between the foreshocks and background seismicity or earthquake swarms, the present results may be useful for distinguishing them.

CHAPTER 7

Concluding Remarks

Through the analyses of waveform and spectrum for the earthquake swarm, foreshock and ordinary seismic activities, some differences of the activity mode among these activities were found. The most striking difference is the "similarity of waveform". The earthquake swarm activity in a certain time interval consists mainly of events with similar waveforms belonging to an earthquake family, though their frequency contents depend on the earthquake size. The epicenters

of earthquakes in a family ($M_{max} \cong 3$) are distributed within a linear dimension of a few hundred meters, suggesting that they occurred on the same fault plane. When the activity was high, another family appeared in an adjacent area separating at most about 1.5 km ($\Delta t_{S-P} \leqq 0.2$ sec) after the activity of the initial family finished. Several families (maximum of five families) are observed for the sequence lasting about one hour.

On the other hand, the foreshock activity consists of events with an individual waveform character. Similarly, the rate of the occurrence of earthquake families is very low in ordinary seismic activities.

The source spectra of the earthquake swarms also show some features differing from those of other activities. The locus of corner frequencies of the events in a given family shows a straight line with a constant corner frequency. This line implies a constant fault area independent of the earthquake size. On the other hand, the corner frequencies of foreshocks differ from one event to another even for events of similar size, and there is no simple linear relationship between the corner frequency and the earthquake size. Such results suggest that an earthquake swarm occurs on the same fault plane as a repeated slipping or a repeated incomplete rupture and foreshocks occur independently in a wide area presumably selecting the place where the rupture strength is relatively low. This may be understandable also by the difference of the stress field between two activities, that is, the earthquake swarm occurs in an area where the tectonic stress is concentrated locally, but the foreshocks occur under the stress concentration over a wide area supposedly including the entire focal area of the main shock.

The earthquake swarm usually does not include extremely large earthquakes (MOGI, 1963b). The earthquake swarms studied here are consistent with Mogi's results, except for the 1980 earthquake swarm of the Izu Peninsula with a different activity mode. The reason for the absence of an extremely large earthquake may be partly due to the limited available stress drop. As mentioned above, the corner frequencies of familiar earthquakes are nearly constant, and their values depend on the size of the largest earthquake within the family. This behavior suggests that the stress drop of the events in each family increases with the earthquake size. However, the stress drop cannot increase indefinitely, and the size of the largest event is controlled by the stress drop or the amount of slip depending on the fault size. Our estimation of the maximum stress drop is about 80 bars for $M=3$ and about 650 bars for $M=4.6$ earthquakes, respectively. In other words, the corner frequency in a family may play an important role for the determination of the largest earthquake. The

largest earthquake in a given family usually occurs in the later stage of its sequence. Continuous monitoring of waveforms and spectra therefore suggests the possibility of predicting the largest event in a given swarm sequence.

Besides the facts mentioned above, the activities directly associated with the extremely large earthquake ($M=6.7$) during the 1980 earthquake swarm of the Izu Peninsula were quite different from those of other sequences. They showed the activity mode of the main shock-aftershocks type and no earthquake family was observed. There are some arguments as to whether the seismic activities preceding the M6.7 earthquake were foreshocks or an earthquake swarm. Considering the difference of activity mode between the two activities, we may conclude that they were the earthquake swarm, because they showed a regular activity mode which differs from that of foreshock activity. Therefore, our method cannot be applicable in the prediction of the occurrence of such a specially large earthquake during the swarm sequence. However, the possibility of the occurrence of a specially large earthquake during a swarm sequence is very low, and it might depend on the seismic region.

When the seismic activity is increasing in a certain region, it is very important to distinguish whether these earthquakes are foreshocks preceding a large earthquake or earthquake swarms without a large earthquake. The difference in the frequency-magnitude relationship (b-value) may be one of the most useful methods for distinguishing foreshocks from other activities. However, the data over fairly long-time interval must be accumulated to obtain a reliable b-value. If our findings presented in this study are applicable for other sequences, they may be useful for distinguishing foreshocks in the early stage of its sequence.

Acknowledgements

I wish to express my deepest gratitude to Professors Kenshiro TSUMURA and Setumi MIYAMURA for their continuous guidance and encouragement given in the course of the present study. I am grateful to Professors Tokuji UTSU, Keiiti AKI, Kunihiko SHIMAZAKI and K. TSUMURA who read the manuscript critically and offered many valuable suggestions and to Dr. Sadaomi SUZUKI for the use of the seismograms of foreshocks obtained in Hokkaido. Discussions with Professors Kiyoo MOGI, Megumi MIZOUE and Mitiyasu OHNAKA were very helpful, and I extend my warmest thanks to them.

This is a part of a *Ph. D. Thesis* submitted to the University of Tokyo.

REFERENCES

AKI, K., 1967, Scaling law of seismic spectrum, *J. Geophys. Res.*, **72**, 1217-1231.

AKI, K., 1969, Analysis of the seismic coda of local earthquakes as scattered waves, *J. Geophys. Res.*, **74**, 615-631.

AKI, K., 1972, Scaling law of earthquake source time-function, *Geophys. G. R. Astr. Soc.*, **31**, 3-25.

AKI, K., 1980a, Attenuation of shear waves in the lithosphere for frequencies from 0.05 to 25 Hz, *Phys. Earth Planet. Inter.*, **21**, 50-60.

AKI, K., 1980b, Scattering and attenuation of shear waves in the lithosphere, *J. Geophys. Res.*, **85**, 6496-6504.

AKI, K. and B. CHOUET, 1975, Origin of coda waves: source, attenuation, and scattering effect, *J. Geophys. Res.*, **80**, 3322-3342.

AKI, K., M. BOUCHON, B. CHOUET and S. DAS, 1977, Quantitative prediction of strong motion for a potential earthquake fault, *Annali di Geofisica*, **15**, 341-368.

BAKUN, W. H. and C. G. BUFE, 1975, Shear-wave attenuation along the San Andreas fault zone in central California, *Bull. Seismol. Soc. Am.*, **65**, 439-459.

BAKUN, W. H. and T. V. MCEVILLY, 1979, Are foreshocks distinctive? Evidence from the 1966 Parkfield and the 1975 Oroville, California sequences, *Bull. Seismol. Soc. Am.*, **69**, 1027-1038.

BARAZANGI, M. and B. ISACKS, 1971, Lateral variations of seismic-wave attenuation in the upper mantle above the inclined earthquake zone of the Tonga Island arc: deep anomaly in the upper mantle, *J. Geophys. Res.*, **76**, 8493-8516.

BRACE, W.F., 1972, Laboratory studies of stick-slip and their application to earthquakes, *Tectonophysics*, **14**, 189-200.

BRUNE, J. N., 1970, Tectonic stress and the spectra of seismic shear waves from earthquakes, *J. Geophys. Res.*, **75**, 4997-5009.

BUFE, C. G., P. W. HARSH and R. O. BURFORD, 1977, Steady-state seismic slip—a precise recurrence model, *Geophys. Res. Lett.*, **4**, 91-94.

CHOUET, B., K. AKI and M. TSUJIURA, 1978, Regional variation of the scaling law of earthquake source spectra, *Bull. Seismol. Soc. Am.*, **68**, 49-70.

CLOWES, R. M. and E. R. KAWASEWICH, 1970, Seismic attenuation and the nature of reflecting horizons within the crust, *J. Geophys. Res.*, **75**, 6693-6705.

DAS, S., 1976, A numerical study of rupture propagation and earthquake source mechanism, *Ph. D. Thesis*, Massachusetts Inst. of Technol., Cambridge.

DAS, S. and K. AKI, 1977, Fault plane with barriers: a versatile earthquake model, *J. Geophys. Res.*, **82**, 5658-5670.

DOUGLAS, B. M. and A. RYALL, 1972, Spectral characteristics and stress drop for microearthquakes near Fairview peak, Nevada, *J. Geophys. Res.*, **77**, 351-359.

ERI, EARTHQUAKE RESEARCH INSTITUTE, 1981, Seismic activities in the Izu Peninsula and its Vicinity (May-October 1980), *Rep. Coordin. Commit. Earthq. Predic.*, **25**, 162-168 (in Japanese).

ESHELBY, J. D., 1957, The determination of the elastic field of an ellipsoidal inclusion and related problems, *Proc. R. Soc. Lond.*, Ser. A, **241**, 376-396.

FEDOTOV, S. A., A. A. GUSEV and S. A. BOLDREV, 1972, Progress of earthquake prediction in Kamchatka, *Tectonophysics*, **14** (3/4), 279-286.

GEDNEY, L., S. ESTES and N. BISWAS, 1980, Earthquake migration in the Fairbanks, Alaska seismic zone, *Bull. Seismol. Soc. Am.*, **70**, 223-241.

HAGIWARA, T. and T. IWATA, 1968, Summary of the seismographic observation of Matsushiro swarm earthquakes, *Bull. Earthq. Res. Inst.*, **46**, 485-515.

HAMAGUCHI, H. and A. HASEGAWA, 1975, Recurrent occurrence of the earthquakes with similar wave forms and its related problems, *Zisin*, **28**, 153-169 (in Japanese).

HORI, M., 1973, Determination of earthquake magnitude of the local and near earthquake

by the Dodaira Microearthquake Observatory, *Speci. Bull. Earthq. Res. Inst.*, **10** (4), 1-4 (in Japanese).

IMAMURA. A., 1913, Report of the earthquake in Summer, 1854, *Rep. Imp. Earthq. Inves. Comm.*, **77**, 1-16 (in Japanese).

IMAMURA, A., 1915, Report of the 1914 Akitaken-Senpokugun earthquake, *Rep. Imp. Earth. Inves. Comm.*, **82**, 1-30 (in Japanese).

ISHIDA, M., 1974, Determination of fault parameters of small earthquakes in the Kii Peninsula, *J. Phys. Earth*, **22**, 177-212.

ISHIDA, M. and H. KANAMORI, 1978, The foreshock activity of the 1971 San Fernando earthquake, California, *Bull. Seismol. Soc. Am.*, **68**, 1265-1279.

ISHIDA, M. and H. KANAMORI, 1980, Temporal variation of seismicity and spectrum of small earthquakes preceding the 1952 Kern County, California earthquake, *Bull. Seismol. Soc. Am.*, **70**, 509-527.

JOHNSON, L. R. and T. V. MCEVILLY, 1974, Near-field observations and source parameters of central California earthquakes, *Bull. Seismol. Soc. Am.*, **64**, 1855-1886.

JOHNSON, C. E. and D. M. HADLEY, 1976, Tectonic implications of th Brawley earthquake swarm, Imperial valley, California, January 1975, *Bull. Seismol. Soc. Am.*, **66**, 1133-1144.

JONES, L. and P. MOLNAR, 1976, Frequency of foreshocks, *Nature*, **262**, 677-679.

KARAKAMA, I., I. OGINO, K. TSUMURA, K. KANJO, M. TAKAHASHI and R. SEGAWA, 1980, The earthquake swarm east off the Izu Peninsula of 1980, *Bull. Earthq. Res. Inst.*, **55**, 913-948 (in Japanese).

KEILIS-BOROK, V.I., 1959, On estimation of the displacement in an earthquake source and of source dimensions, *Ann. Geofis.*, **12**, 205-214.

KLEIN, F. W., P. EINARSSON and M. WYSS, 1977, The Reykjanes Peninsula, Iceland, earthquake swarm of September 1972 and its tectonic significance, *J. Geophys. Res.*, **82**, 865-888.

KURITA, T., 1975, Attenuation of shear waves along the San Andreas fault zone in central California, *Bull. Seismol. Soc. Am.*, **65**, 277-292.

MADARIAGA, R., 1976, The dynamics of an expanding circular fault, *Bull. Seismol. Soc. Am.*, **66**, 639-666.

MASUDA, T., 1978, Distribution of the stress drop of microearthquakes on source depth, *Abstract for Ann. Meet. Seismol. Soc. Japan*, 1, p. 88 (in Japanese).

MITSUNAMI, T. and A. KUBOTERA, 1977, On the activity of the earthquake swarm in the northern part of Aso Caldera, 1975—Interpretation of hypocentral migration—, *Zisin*, **30**, 73-90 (in Japanese).

MIYAMURA, S. and M. TSUJIURA, 1955, A VHF radio telerecording seismograph (abbr. RTS), *Bull. Earthq. Res. Inst.*, **33**, 725-731 (in Japanese).

MIYAMURA, S. and M. TSUJIURA, 1957, UHF multi-channel radio tele-recording seismograph. part 1, *Bull. Earthq. Res. Inst.*, **35**, 381-394 (in Japanese).

MOGI, K., 1963a, The fracture of semi-infinite body caused by an inner stress origin and its relation to the earthquake phenomena (second paper), *Bull. Earthq. Res. Inst.*, **41**, 596-614.

MOGI, K., 1963b, Some discussion on aftershocks, foreshocks and earthquake swarms—the fracture of a semi-infinite body caused by an inner stress origin and its relation to the earthquake phenomena (third paper), *Bull. Earthq. Res. Inst.*, **41**, 615-658.

MOTOYA, Y., 1970, Aftershock sequence of the earthquake east off Hokkaido on August 12, 1969, *Geophys. Bull. Hokkaido Univ.*, **24**, 93-106 (in Japanese).

MOTOYA, Y., S. SUZUKI and T. TAKANAMI, 1979, On earthquake swarm near Hakodate, southern Hokkaido, *Abstract for Ann. Meet. Seismol. Soc. Japan*, **2**, p. 42 (in Japanese).

NASU, N., F. KISHINOUYE and T. KODAIRA, 1931, Recent seismic activities in the Idu Peninsula, (Part 1), *Bull. Earthq. Res. Inst.*, **9**, 22-35.

OKADA, HM., H. WATANABE, H. YAMASHITA and I. YOKOYAMA, 1981, Seismological significance

of the 1977-1978 eruptions and the magma intrusion process of Usu Volcano, Hokkaido, *J. Volcanol. Geotherm. Res.*, **9**, 311-334.

ŌMORI, F., 1910, On the foreshocks of large earthquakes, *Rep. Imp. Earthq. Inves. Comm.*, **68A**, 31-38 (in Japanese).

O'NEILL, M. E. and J. H. HEALY, 1973, Determination of source parameters of small earthquakes from *P*-wave rise time, *Bull. Seismol. Soc. Am.*, **63**, 599-614.

PAPAZACHOS, B. C., 1975, Foreshocks and earthquake prediction, *Tectonophysics*, **28**, 213-226.

PRESS, F., 1964, Seismic wave attenuation in the crust, *J. Geophys. Res.*, **69**, 4417-4418.

RAUTIAN, T. G. and V. I. KHALTURIN, 1978, The use of coda for determination of the earthquake source spectrum, *Bull. Seismol. Soc. Am.*, **68**, 923-948.

SATO, T., S. HORIUCHI, T. SATO, S. HORI and H. ISHII, 1979, Waveform analysis of Iwasaki earthquake swarm, *Abstract for Ann. Meet. Seismol. Soc. Japan*, **2**, p. 45 (in Japanese).

SATO, H. and S. MATSUMURA, 1980, Q^{-1} value for *S*-waves (2-32 Hz) under the Kanto district in Japan, *Zisin*, **33**, 541-543 (in Japanese).

SBAR, M. L., J. ARMBRUSTER and Y. P. AGGARWAL, 1972, The Adirondack, New York, earthquake swarm of 1971 and tectonic implications, *Bull. Seismol. Soc. Am.*, **62**, 1303-1317.

SCHOLZ, C. H., 1968, The frequency-magnitude relation of microfracturing in rocks and its relation to earthquakes, *Bull. Seismol. Soc. Am.*, **58**, 399-415.

SHIMAZAKI, K. and T. NAKATA, 1980, Time-predictable recurrence model for large earthquakes, *Geophys. Res. Lett.*, **7**, 279-282.

STAUDER, W. and A. RYALL, 1967, Spatial distribution and source mechanism of microearthquakes in central Nevada, *Bull. Seismol. Soc. Am.*, **57**, 1317-1345.

SUMNER, R. D., 1967, Attenuation of earthquake generated *P*-waves along the western Flank of the Andes, *Bull. Seismol. Soc. Am.*, **57**, 173-190.

SUYEHIRO, S., 1966, Difference between aftershocks and foreshocks in the relationship of magnitude to frequency of occurrence for the great Chilean earthquake of 1960, *Bull. Seismol. Soc. Am.*, **56**, 185-200.

SUYEHIRO, S., 1969, Difference in the relationship of magnitude to frequency of occurrence between aftershocks and foreshocks of an earthquake of magnitude 5.1 in central Japan, *Pap. Met. Geophys.*, **20**, 157-187.

SUYEHIRO, S., T. ASADA and M. OHTAKE, 1964, Foreshocks and aftershocks accompanying a perceptible earthquake in central Japan, *Pap. Met. Geophys.*, **15**, 71-88.

SUZUKI, S., 1981, Foreshock activity of the earthquake (*M* 5.4) off cape Erimo on January 19, 1979, *Zisin*, **34**, 269-272 (in Japanese).

SYLVESTER, A. G., S. W. SMITH and C. H. SCHOLZ, 1970, Earthquake swarm in the Santa Barbara channel, California, 1968, *Bull. Seismol. Soc. Am.*, **60**, 1047-1060.

TANAKA, T., M. SAKAUE, Y. OSAWA and S. YOSHIZAWA, 1980, Strong-motion accelerograms and maximum acceleration data of the Izu-Hanto-Toho-Oki earthquake and the swarm earthquakes of 1980, *Bull. Earthq. Res. Inst.*, **55**, 1043-1064 (in Japanese).

TERASHIMA, T., 1968, Magnitude of microearthquake and the spectra of microearthquake waves, *Bull. Internat. Inst. Seism. and Earthq. Eng.*, **5**, 31-108.

THATCHER, W., 1972, Regional variations of seismic source parameters in the northern Baja California area, *J. Geophys. Res.*, **77**, 1549-1565.

THATCHER, W. and T. C. HANKS, 1973, Source parameters of southern California earthquakes, *J. Geophys. Res.*, **78**, 8547-8576.

TSUJIURA, M., 1963, Multi-channel triggered magnetic tape recording for routine seismic observation. Part 1, *Bull. Earthq. Res. Inst.*, **41**, 419-445 (in Japanese).

TSUJIURA, M., 1965, A pen-writing long-period seismograph, Part 3, *Bull. Earthq. Res. Inst.*, **43**, 479-440 (in Japanese).

TSUJIURA, M., 1966, Frequency analysis of seismic waves (1), *Bull. Earthq. Res. Inst.*, **44**, 873-891.

TSUJIURA, M., 1967, Frequency analysis of seismic waves (2), *Bull. Earthq. Res. Inst.*, **45**, 973-995.

TSUJIURA, M., 1969, Regional variation of *P* wave spectrm (1), *Bull. Earthq. Res. Inst.*, **47**, 613-633.

TSUJIURA, M., 1972, Spectra of body waves and their dependence on source depth 1, Japanese arc, *J. Phys. Earth*, **20**, 251-266.

TSUJIURA, M., 1973a, Regional variation of micro-earthquake spectrum, *Zisin*, **26**, 370-375 (in Japanese).

TSUJIURA, M., 1973b, Spectrum of seismic waves and its dependence on magnitude (1), *J. Phys. Earth*, **21**, 373-391.

TSUJIURA, M., 1977, Spectral features of foreshocks, *Bull. Earthq. Res. Inst.*, **52**, 357-371.

TSUJIURA, M., 1978a, Spectral analysis of the coda waves from local earthquakes, *Bull. Earthq. Res. Inst.*, **53**, 1-48.

TSUJIURA, M., 1978b, Spectral analysis of seismic waves for a sequence of foreshocks, main shock and aftershocks: the Izu-Oshima-kinkai earthquake of 1978, *Bull. Earthq. Res. Inst.*, **53**, 741-759 (in Japanese).

TSUJIURA, M., 1979a, Mechanism of the earthquake swarm activity in the Kawanazaki-oki, Izu Peninsula, as inferred from the analysis of seismic waveforms, *Bull. Earthq. Res. Inst.*, **54**, 441-462.

TSUJIURA, M., 1979b, The difference between foreshocks and earthquake swarms, as inferred from the similarity of seismic waveform (Preliminary report), *Bull. Earthq. Res. Inst.*, **54**, 309-315 (in Japanese).

TSUJIURA, M., 1980, Earthquake swarm activity in the northern Tokyo Bay, *Bull. Earthq. Res. Inst.*, **55**, 601-619.

TSUJIURA, M., 1981, Activity mode of the 1980 earthquake swarm off the east coast of the Izu Peninsula, *Bull. Earthq. Res. Inst.*, **56**, 1-24.

TSUJIURA, M. and S. MIYAMURA, 1959, UHF multi-channel radio tele-recording seismograph, Part II, *Bull. Earthq. Res. Inst.*, **37**, 193-206 (in Japanese).

TSUKUDA, T., 1980, Source process of microearthquakes deduced from *P* waveforms Part II, Source parameters and the structure of the fractured region within the crust, preprint.

TSUMURA, K., 1973, Microearthquake activity in the Kanto district, Pub. 50th Anniversary of the great Kanto earthquake, 1923, *Earthq. Res., Inst.*, 67-87 (in Japanese).

TSUMURA, K., I KARAKAMA, I. OGINO, K. SAKAI and M. TAKAHASHI, 1977, Observation of the earthquake swarm in the Izu Peninsula (1975-1977), *Bull. Earthq. Res. Inst.*, **52**, 113-140 (in Japanese).

TSUMURA, K., I. KARAKAMA, I. OGINO and M. TAKAHASHI, 1978, Seismic activities before and after the Izu-Oshima-kinkai earthquake of 1978, *Bull. Earthq. Res. Inst.*, **53**, 675-706 (in Japanese).

TSUMURA, K., I. KARAKAMA, I. OGINO, M. TAKAHASHI, I. NAKAMURA and K. KANJO, 1979, Earthquake swarm off Kawanazaki, Izu Peninsula, *Abstract for Ann. Meet. Seismol. Soc. Japan*, **1**, p. 38 (in Japanese).

UCHIIKE, H. and M. ICHIKAWA, 1976, On the earthquake of the eastern part of Yamanashi Prefecture, June 16, 1976, *Abstract for Ann. Meet. Seismol. Soc. Japan*, **2**, p. 18 (in Japanese).

UTSU, T., 1969, Aftershocks and earthquake statistics (1), *J. Faculty of Science, Hokkaido Univ.*, Ser. VII, **3**, 129-185.

UTSU, T., 1970, Aftershocks and earthquake statistics (II), *J. Faculty of Science, Hokkaido Univ.*, Ser. VII, **3**, 197-266.

UTSU, T., 1971, Aftershocks and earthquake statistics (III), *J. Faculty of Science, Hokkaido Univ.*, Ser. VII, **3**, 379-441.

UTSU, T., 1981, Seismicity of the Izu Peninsula and its vicinity from 1901 through 1980 with some remarks on the characteristics of foreshock activitics, *Bull. Earthq. Res. Inst.*, **56**, 25-41.

WANO, K. and HM. OKADA, 1980, Peculiar occurrence of Usu earthquake swarm associated with the recent doming activity, *Zisin*, **33**, 215-226 (in Japanese).

WETMILLER, R. J., 1971, An earthquake swarm on the Queen Charlotte Islands fracture zone, *Bull. Seismol. Soc. Am.*, **61**, 1489-1505.

WYSS, M. and J. N. BRUNE, 1971, Regional variations of source properties in southern California estimated from the ratio of short- to long-period amplitudes, *Bull. Seismol. Soc. Am.*, **61**, 1153-1167.

YAMAKAWA, N., 1966, Foreshocks, aftershocks and earthquake swarms (1) A definition of foreshocks, aftershocks and earthquake swarms and its application to seismicity, *Pap. Met. Geophys.*, **17**, 157-189.

YAMAKAWA, N., 1967a, Foreshocks, aftershocks and earthquake swarms (II) Areal characteristics of abnormal seismic activities, *Pap. Met. Geophys.*, **18**, 15-26.

YAMAKAWA, N., 1967b, Foreshocks, aftershocks and earthquake swarms (III) Detailed areal characteristics of aftershock activities, *Pap. Met., Geophys.*, **18**, 77-88.

YAMAKAWA, N., A. YOSHIDA and M. KISHIO, 1979, Space-time distribution of foreshocks and aftershocks of the Izu-Oshima-Kinkai earthquake of 1978—in relation to tectonics in and around the Izu Peninsula—, *Zisin*, **32**, 89-101 (in Japanese).

ZHENG, J., 1981, Precursors to the Haicheng and Tangshan earthquakes, *Zisin*, **34**, 43-59 (in Japanese).

3. 群発地震と前震の波形及びスペクトル特性

——地震予知に関連して——

地震研究所　辻浦　賢

ある地域における地震活動が活発化した場合，それが群発地震であるか，前震であるかを識別することは地震学的にも，又地震予知の見地からも極めて重要な問題である．

ここでは，群発地震についての波形，並びにスペクトル解析から，群発地震のもつ特徴を明らかにすると共に，同様な解析を前震活動にも適用し，両者の性質の違いを見出そうとするものである．

対象とした地域は関東地方である．堂平観測所並びにその衛星観測所の資料から，過去 14 年間で 15 個の群発地震，及び 3 個の前震活動を選び，それぞれの波形解析及びスペクトル解析を行なった．

I. 群発地震の波形解析

早送り記録の重ね合わせにより波形について調べた結果:

1. ある時間帯（活動度により異なる）に発生する地震は非常に似かよった波形を示し，所謂“相似地震”によって構成される．
2. 一連の相似地震の活動が終ると，別の相似地震群が隣接地域において発生する（活動が高い場合）．
3. 相似地震の震源域は数百米である（$M_{max}\approx 3$）．
4. 相似地震に含まれる最大地震は，その系列の後半に発生する．

II. 群発地震のスペクトル解析

アナログ型バンドパスフイルターの記録を用い，それぞれの相似地震群の震源スペクトルを求めた．主な結果は:

1. 相似地震のコーナー周波数は，ある範囲の地震（$\Delta M\approx 2$）に対し略一定である．
2. ある相似地震のコーナー周波数は，その地震群に含まれる最大地震の大きさに依存する．
3. 従って，相似地震に含まれる最大地震の大きさはストレスドロップ量（スベリ量）によって制限される．

III. 前震の波形及びスペクトル解析

群発地震で用いた同じ方法により，前震活動及び一部定常活動の地震についても解析を行なった．主な結果は:

1. 前震はそれぞれ独立した波形を持ち，群発地震で見られたような相似地震は現われない．
2. 前震活動におけるそれぞれの地震のコーナー周波数は複雑に分布し，群発地震でみられたような地震の大きさ（モーメント）と震源の大きさとの間で単純な直線関係は見られない．
3. 定常活動における相似地震の発生率は極めて低い．

以上，群発地震，前震及び定常活動における地震について，それぞれの活動様式の特徴を明らかにした．この様な特徴はそれぞれの地震群の発生様式の違いに起因するものであろうと推定される．すなわち，群発地震は局所的な応力集中の場で発生し，そのため極めてせまい範囲おそらく同じ断層面上で，繰り返し発生するのに対し，前震は，広域応力場での発生のため，広範囲の領域で発生したことを反映したものであろう．従って，若しこの様な違いが，他の前震及び群発地震についても適用されるならば，地震波形並びにスペクトルの連続的な監視が地震予知のための１資料として役立つことが期待される．